J Mol Model (2013) 19:3279–3305
DOI 10.1007/s00894-013-1858-0

ORIGINAL PAPER

A theoretical investigation on the proton transfer tautomerization mechanisms of 2-thioxanthine within microsolvent and long range solvent

Hong-Jiang Ren · Ke-He Su · Yan Liu · Xiao-Jun Li · Jun Xiao · Yan-Li Wang

Received: 20 February 2013 / Accepted: 17 April 2013 / Published online: 8 May 2013

Abstract A relative complete study on the mechanisms of the proton transfer reactions of 2-thioxanthine was carried out with density functional theory. The models were designed with monohydrated and dihydrated microsolvent catalyses either with or without the presence of water solvent considered with the polarized continuum model (PCM). A total number of 114 complexes and 67 transition states were found with the B3LYP/6-311+G** calculations. The energies were refined with both B3LYP/aug-cc-pVTZ and PCM-B3LYP/aug-cc-pVTZ methods. The activation energies were reported with respect to the Gibbs free energies obtained in conjunction with the standard statistical thermodynamics. Possible reaction pathways were confirmed with the intrinsic reaction coordinates. Pathways *via* C8 atom on the imidazole ring, *via* the bridged C4 and C5 atoms between pyrimidine and imidazole rings and *via* N, O and S atom on the pyrimidine ring were examined. The results show that the most feasible pathway is the proton transfers within the long range solvent surrounding *via* the N, O and S atoms in the pyrimidine ring with di-hydrated catalysis: N(7)H+2H_2O→IM89→IM90→P13+2H_2O→IM91→IM92→P6+2H_2O→IM71→IM72→P7+2H_2O→IM107→IM108→P18+2H_2O→IM111→IM112→P19+2H_2O→IM113→IM114→P17+2H_2O→IM105→IM106→N(9)H+2H_2O that has the highest energy barrier of 44.0 kJ mol^{-1} in the transition of IM89 to IM90 *via* TS54. The small energy barrier is in good agreement with the experimental observation that 2-TX tautomerizes at room temperature in water. In the aqueous phase, the most stable intermediate is found to be IM21 [**N(7)H**+2H_2O] and the possible co-existing species are the monohydrated IM1, IM9, IM39 and IM46, and the di-hydrated IM5, IM8, IM13, IM16, IM81, IM89, IM90, IM91 and IM106 complexes that have a relative concentration larger than 10^{-6} (1 ppm) with respect to IM21.

Keywords Proton transfer · Solvent effects · Tautomerization · 2-thioxanthine

Introduction

2-thioxanthine (2TX), a DNA base analog, evoked intensive interests in recent years [1–5] mainly due to the discovery of its valuable pharmacological properties of acting as a potential inhibitor of *E. coli* Fpg protein (formamidopyrimidine–DNA glycosylase) [2], an anticancer reagent [3, 4] and a deactivation reagent to xanthine [5]. This molecule was found easy to isomerize with respect to a hydrogen atom transferring among the atoms on the pyrimidine and the imidazole rings both experimentally [6, 7] and theoretically [1]. The biological activities are quite different for different tautomers [2]. It is possible that there are three kinds of tautomerizations: **N(7)H↔N(9)H**, keto↔enol and thione↔thiol. The experiments found that the tautomers **N(7)H** and **N(9)H** are the co-existing species in both gaseous and aqueous phase [6, 7]. The stability order of other 12 possible tautomers were only predicted theoretically [8, 9]. The theoretical investigations also

Electronic supplementary material The online version of this article (doi:10.1007/s00894-013-1858-0) contains supplementary material, which is available to authorized users.

H.-J. Ren · K.-H. Su (✉) · Y. Liu · X.-J. Li · J. Xiao · Y.-L. Wang
Key Laboratory of Space Applied Physics and Chemistry of the Ministry of Education, School of Natural and Applied Sciences, Northwestern Polytechnical University, Xi'an, Shaanxi 710072, People's Republic of China
e-mail: sukehe@nwpu.edu.cn

H.-J. Ren
College of Chemistry and Chemical Engineering, Xi'an University of Arts and Science, Xi'an, Shaanxi 710065, People's Republic of China

found that the **N(7)H** tautomer is more stable than **N(9)H** either in the gaseous or in the aqueous phase, which is consistent with the experimental observations [6, 7]. It is interesting that ref. [2] revealed that only the **N(9)H** form exhibited the most efficient inhibiting activity toward 2,6-diamino-4-hydroxy-5N-methyl-formamidopyrimidine (Fapy- 7MeG) over 17 analogs of purine compounds. Therefore, the mechanism of **N(7)H** to **N(9)H** tautomerization reactions need to be investigated in detail.

Our previous study [1] reported theoretically the reaction mechanisms of the intramolecular proton transfer in the gas phase, where the solvent molecule(s) or the solvent surrounding was not involved, and found that there are three paths associated with imidazole ring and nine rate-determining barriers associated with pyrimidine ring. However, the solvent is especially important for the hydration being a universal phenomenon in the biological processes [10–17], and always plays the role of a catalyst [18–25]. For example, Kastas [18] found that the solvent media would lead the tautomerism reaction of (E)-2-[(4-fluorophenyl)iminomethyl]-5- methoxyphenol to occur easier than in the gas phase using FT-IR spectrum and UV-vis absorption spectra. Iglesias [19] observed that the activation energy for the ketonization reaction decreases for the keto-enol tautomerism of 2-acetylcyclohexanone(ACHE) in water. Even for the reduction reaction of the simple molecule formic acid, Shen *et al*. [20] found that water molecules might participate as a catalyst in the transition state by forming a hydrogen-bond ring network. Theoretically, Ahn *et al*. [22] found that the participation of water molecule in the tautomerization of purine will dramatically lower the reaction barrier. It is interesting that their work also found that two or three water molecules reduce the activation energy by almost the same magnitude. Kim *et al*. [23] found that one or two water molecules (as microsolvation) will tremendously decrease the barrier of the tautomerization of adenine. Similarly, Okovytyy *et al*. [24] found that one or two ethanol molecules can reduce the barriers of the tautomerization reactions of 1,3-dihydro-2H-1,5-benzodiazepin-2-ones (or -2-thiones) but the bulk of solvent does not substantially change the barriers or the equilibrium constants for the ethanol-assisted reactions. In the present molecule, Yuan *et al*. [25] reported that one water molecule may result in different hydrated 2-thioxanthine (2TX) N(7)H complexes with different stabilities. In contrast in some cases, water molecule would not always accelerate the reaction. For example, Balta *et al*. [26, 27] found that the activation energy of the proton transfer of glycine in the presence of water molecules is higher than that of the isolated molecule.

Obviously, it is interesting to examine the tautomerization reaction mechanisms within solvent surroundings and to look into the insights of the reaction pathways. To our knowledge, the water-assisted proton transfer reaction mechanisms for the 2-thioxanthine tautomerizations (*i.e.*, reaction paths and the energy barriers) have not been studied experimentally or theoretically.

The present work will carry out a theoretical study on the intramolecular proton transfer reactions of 2TX in monohydrated and dihydrated forms to determine the reaction energy barriers and try to explore all the possible paths of the reactions. The long-range solvent effects will also be examined.

Computational details

All the calculations were performed by using the Gaussian-09W program [28] and the density functional theory (DFT) of B3LYP method [29] was chosen. This is due to the functional has been widely used in the study of tautomerisms of heterocyclic compounds to provide the correct molecular geometries, activation energies and energy differences between pairs of tautomers [30–33]. The long-range solvent effects will be involved by employing the polarized continuous model (PCM) [34–38].

All the geometries of the reactants, transition states (TS), intermediates and the products were optimized with B3LYP/6-311+G** [29]. Frequency analyses at the same level of theory were followed with the optimized geometries to determine the harmonic vibrational frequencies and to confirm the structure being a stable species (without imaginary frequency) or a transition state (with solely an imaginary frequency). The intrinsic reaction coordinates (IRC) for both forward and reverse directions started at each TS were also searched to confirm the correct connections. The molecular energies were further refined with a higher level (larger basis sets) method B3LYP/aug-cc-pVTZ by using the B3LYP/6-311+G** geometries. The geometries of the microsolvent models would also be approximately used in the solution due to difficulties of convergence would always be encountered in the geometry optimizations of a TS within the PCM model. This treatment was tested with the energies of a path, **P(4)** as being discussed in the next section, and the results show that the two energy barriers in the path are slightly different by only 3.4 and 6.2 kJ mol^{-1}. Actually, investigations have also shown similar negligible difference on the molecular structure in the long-range solvent [30–33].

The standard (100 kPa) Gibbs free energies of the 114 complexes and 67 transition states at 298.15 K were evaluated in conjunction with the standard statistical thermodynamics by using the B3LYP/6-311+G** geometries and the scaled (by a factor of 0.9688 [39]) frequencies. The Gibbs free energy in the solution is directly obtained from the PCM calculations. Figure 1 illustrates the atomic numbering

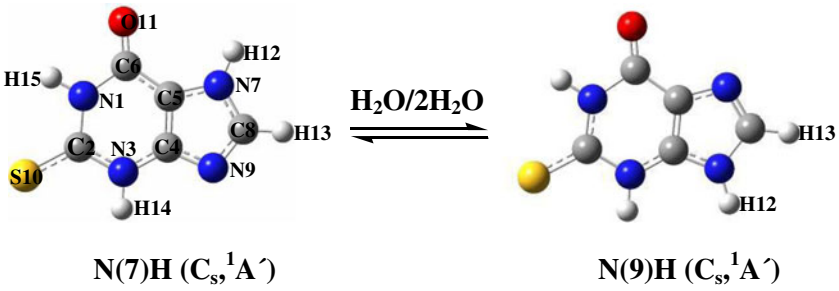

Fig. 1 Atomic numbering and the structure of **N(7)H** and **N(9)H** tautomers of 2-thioxanthine

of the **N(7)H** and **N(9)H** tautomers, which is consistent with that in refs. [1, 8, 9] for the convenience of compassions.

Results and discussion

The relative Gibbs free energies for the species of mono- and di-hydration reactions both for the microsolvent models and in the aqueous phases are listed in Tables 1, 2, 3, 4 and 5. The calculated electronic energy and Gibbs free energy are given in Supplement 1, 2 and 3. The zero point energy, electronic energy, relative energy and the imaginary frequency of the transition state are summarized in Supplement 4, 6 and 7. The stable Gibbs energy of eleven monohydrated and di-hydrated relative species are shown in Supplement 5.

Proton transfer via C8 tetrahedral complexes in the imidazole ring

Pathway P(1) **P(1)** is associated with one water molecule as shown in Fig. 2 within which panel (a) is the evolution of the molecular structures and (b) is the energy profile.

A water molecule interacts first with the isolated reactant 2TX (denoted as **N(7)H**) to produce an intermediate IM1 with the formation of two intermolecular hydrogen bonds. One of these bonds is between O11 and H17 with a distance of 1.871 Å and the other is between H12 and O16 with 1.862 Å. In IM1, the O16 and H17 atoms of the water molecule are almost in the molecular plane of **N(7)H**. It is shown in Table 1 that IM1 is the most stable complex in the mono-hydrated pathway **P(1)**, which is consistent with the prediction of ref. [25]. This process is associated with an energy (Gibbs free energy at 298.15 K) release of 14.2 kJ mol^{-1}. It is notable that the relative thermodynamic energy at 0 K is 41.3 kJ mol^{-1} (Supplement 4), a typical value of two hydrogen bonds.

The next step is that the water molecule moves onto the imidazole ring above N7-C8 bond from the purine ring plane and forms a five-member ring transition state TS1 with an energy barrier of 268.8 kJ mol^{-1}. It is clear by examination of the normal mode of the imaginary vibration that a concert double proton transferring mechanism is followed. The hydrogen atom H18 in the water molecule transfers onto the C8 atom and the hydrogen atom H12 attaching N7 of the imidazole ring shifts onto the O16 atom of the water molecule. The larger activation energy should mainly be from the bond breaking of the N7-H12 bond, which is the key step in the tautomerizations. However, this barrier is higher than the value 209.9 kJ mol^{-1} obtained previously with the G3(MP2) [1] calculations without the existence of the water molecule, implying that the pathway **P(1)** is less feasible.

Once TS1 is formed, an intermediate IM2 may be produced with an energy release of 148.4 kJ mol^{-1}. In this process, C8 atom in IM2 is saturated with four sp^3–type bonds (*i.e.*, two C-H and two C-N single bonds) associated with the formation of a hydrogen bond between N7 and H12 atoms with the distance of 2.041 Å. IM2 is actually a complex of a water molecule and an unstable tautomer of 2TX that is 100.7 kJ mol^{-1} higher in energy than the reactant.

The water molecule would spontaneously dissociate from the complex to produce tautomer P1 due to a negative (−5.5 kJ mol^{-1}) Gibbs free energy change. This process is associated with a thermodynamic energy (at 0 K) increase of 15.3 kJ mol^{-1}. Obviously, the dissociation of the water molecule is a process of increasing entropy that will result in a decrease of the Gibbs free energy.

Additional tautomerization of P1 is possible where a water molecule may interact with P1 and form a hydrogen bond between N9 and H12 (with a distance of 2.029 Å) to produce a complex IM3. This process is associated with a decrease in energy (−13.6 kJ mol^{-1}) but slightly increase in Gibbs free energy (6.9 kJ mol^{-1}) due to entropy decreasing.

IM3 may isomerize into IM4 *via* another five-member ring (C8-N9-H12-O16-H17) transition state TS2 with an energy barrier of 163.5 kJ mol^{-1}. In TS2, the water molecule is located above the plane of the imidazole ring and the H17 atom interacts strongly with the O atom of the water molecule that leads to the breaking of the C8-H17 bond. The H12 atom of the water molecule interacts strongly with the N9 atom and finally forms a N9-H12 bond that results in the H transfer. This is a process of H exchange with the assistant of the water molecule (*i.e.*, bonding H17 and releasing H12). At this point, an expected intermediate should be

formed. However, the IRC calculations failed to terminate. Instead, the water molecule attaching H12 moved significantly toward H14 to form the stable complex, IM4, a complex of the aimed product **N(9)H** and a water molecule combined by two hydrogen bonds with a thermodynamic energy of 28.1 kJ mol^{-1} at 0 K. The Gibbs free energy of IM4 is 48.0 kJ mol^{-1} higher than the reactant complex IM1 (Table 1 and Supplement 5) that predicts IM4 can only be in a low concentration of 3.9×10^{-9} at 298.15 K estimated with $\Delta G=-RT\ln K_T$ in case the concentration of IM1 is 1, the reference value. However, the concentration is increased to 1.8×10^{-4} (ΔG=21.4 kJ mol^{-1}) by considering the long range solvent indicating that IM4 can coexist with IM1 if no other even more stable species can be found. However, in the later discussions, the energy of the two water reference (IM21) is found 19.7 kJ mol^{-1} lower than that of IM1. This corresponds to the relative concentration of IM1 being 3.5×10^{-4} implying that IM1 can also be observable in the experiment, but that of IM4 being 6.3×10^{-8} (*e.g.*, less than 1 ppm), a difficult value to be detected.

Figure 2 also shows that the water molecule may easily leave IM4 with a small increase of the Gibbs free energy of 3.5 kJ mol^{-1} (or an internal energy of 28.1 kJ mol^{-1} as presented above) to produce the isolated **N(9)H** tautomer.

These results indicate that the rate-determining step of the pathway **P(1)** is the transition of IM1 to TS1 that has a higher activation energy barrier of 268.8 kJ mol^{-1}. After considering the long-range solvent effect using the PCM model, this value is reduced to 216.6 kJ mol^{-1}, showing that the long-range solvent effect may play an important role in the tautomerization reactions.

Pathway P(2) **P(2)** is a similar process as **P(1)** but is associated with two water molecules as shown in Fig. 3.

Two water molecules may first interact with the isolated reactant **N(7)H** to produce a complex intermediate IM5 with the formation of three intermolecular hydrogen bonds. One is between the two water molecules and two are between the mother molecule **N(7)H** and a water molecule. The distances are within the region of a typical hydrogen bond, *i.e.*, 1.889 Å for O20-H18, 1.976 Å for O11-H17 and 1.782 Å for O16-H12. The data in Table 1 also show that IM5 is the most stable species in the di-hydration complexes. Its formation is associated with a Gibbs free energy release of 7.8 kJ mol^{-1} at 298.15 K. As has been expected that the relative thermodynamic energy at 0 K is 55.6 kJ mol^{-1} (Supplement 6), also a typical value of the summation of three hydrogen bonds.

The following step is that the two water molecules move onto the imidazole ring above N7-C8 bond from the purine ring plane and form a seven-member ring transition state TS3 with an energy barrier of 202.5 kJ mol^{-1}. The normal mode of the imaginary vibration corresponds to a concert triple proton transfer mechanism where the hydrogen atom H19 in one water transfers onto the C8 atom and the hydrogen H12 attaching N7 of the imidazole ring shifts onto the O16 atom of another water molecule. The barrier is lower than that (268.8 kJ mol^{-1}) in pathway **P(1)**, showing that two water molecules facilitate the proton transfer and effectively catalyze the process.

Following TS3, an intermediate IM6 may be produced with an energy release of 81.7 kJ mol^{-1}. In this process, the C8 atom in IM6 is again saturated with four sp^3-type bonds (similar to that in **P(1)**) associated with the formation of three hydrogen bonds between the two water molecules and

Table 1 Relative Gibbs free energies (ΔG in kJ mol^{-1} at 298.15 K)[a] for the species of mono- and di-hydration reactions for **P(1)** and **P(2)** calculated with B3LYP/Aug-cc-pVTZ//B3LYP/6-311+G**

Mono-hydrated	ΔG[b]	Di-hydrated	ΔG[c]
N(7)H+H_2O	0.0 (0.0)	N(7)H+2H_2O	0.0 (0.0)
IM1	−14.2 (−7.9)	IM5	−7.8 (−18.3)
TS1	254.6 (208.7)	TS3	194.7 (159.5)
IM2	106.2 (124.7)	IM6	113.0 (113.1)
P1+H_2O	100.7 (126.5)	P1+2H_2O	100.7 (126.5)
IM3	107.6 (123.4)	IM7	114.2 (110.8)
TS2	271.1 (218.1)	TS4	209.8 (151.3)
IM4	33.8 (13.5)	IM8	17.5 (4.2)
N(9)H+H_2O	37.3 (12.6)	N(9)H+2H_2O	37.3 (12.6)

[a] Energy in the parentheses is for the aqueous phase

[b] Relative Gibbs free energy with respect to **N(7)H+H_2O** for mono-hydration

[c] Relative Gibbs free energy with respect to **N(7)H+2H_2O** for di-hydration

Table 2 Relative Gibbs free energies (ΔG in kJ mol^{-1} at 298.15 K)[a] for the species of mono- and di-hydration reactions for **P(3)** and **P(4)** calculated with B3LYP/Aug-cc-pVTZ//B3LYP/6-311+G**

Mono-hydrated	ΔG[b]	Di-hydrated	ΔG[c]
N(7)H+H_2O	0.0 (0.0)	N(7)H+2H_2O	0.0 (0.0)
IM9	9.6 (0.0)	IM13	9.8 (−15.8)
TS5	229.7 (208.5)	TS7	169.5 (104.8)
IM10	131.5 (114.7)	IM14	111.8 (85.2)
P2+H_2O	133.1 (111.3)	P2+2H_2O	133.1(111.3)
IM11	137.6 (114.0)	IM15	123.2 (85.5)
TS6	252.0 (215.8)	TS8	186.4 (105.8)
IM12	39.9 (8.0)	IM16	39.8 (−4.3)
N(9)H+H_2O	37.3 (12.6)	N(9)H+2H_2O	37.3 (12.6)

[a] Energy in the parentheses is for the aqueous phase

[b] Relative Gibbs free energy with respect to **N(7)H+H_2O** for mono-hydration

[c] Relative Gibbs free energy with respect to **N(7)H+2H_2O** for di-hydration

Table 3 Relative Gibbs free energies (ΔG in kJmol^{-1} at 298.15 K)[a] for the species of mono- and di-hydration reactions for **P(5)** and **P(6)** calculated with B3LYP/Aug-cc-pVTZ//B3LYP/6-311+G**

Mono-hydrated	ΔG[b]	Di-hydrated	ΔG[c]
N(7)H+H_2O	0.0 (0.0)	N(7)H+2H_2O	0.0 (0.0)
IM1	−14.3 (−7.9)	IM21	−20.2 (−27.6)
TS9	237.4 (204.5)	TS12	183.8 (135.3)
IM17	125.4 (133.6)	IM22	123.4 (117.3)
P3+H_2O	117.6 (129.8)	P3+2H_2O	117.6 (129.8)
IM18	126.2 (132.2)	IM23	127.8 (134.2)
TS10	261.9 (250.5)	TS13	262.3 (251.0)
IM19	181.4 (193.7)	IM24	183.1 (196.1)
P4+H_2O	171.1 (189.7)	TS14	287.0 (265.4)
IM20	181.1 (196.6)	IM25	20.8 (8.7)
TS11	287.2 (263.2)	N(9)H+2H_2O	37.3 (12.6)
IM4	33.8 (13.5)		
N(9)H+H_2O	37.3 (12.6)		

[a] Energy in the parentheses is for the aqueous phase

[b] Relative Gibbs free energy with respect to **N(7)H+H_2O** for mono-hydration

[c] Relative Gibbs free energy with respect to **N(7)H+2H_2O** for di-hydration

the product P1 with the distances of 2.210, 1.867 and 1.979 Å. IM6 is also a complex of two water molecules and an unstable tautomer P1 which is the same as that in **P(1)**.

The water molecules would also spontaneously leave the complex to produce the tautomer P1 due to a negative (−12.3 kJ mol^{-1}) Gibbs free energy change. This process is associated with a thermodynamic energy (at 0 K) increase of 37.9 kJ mol^{-1}.

Similar to **P(1)**, an additional tautomerization occurs where the two water molecules may also interact with P1 and form three hydrogen bonds with the distances of 2.204, 1.875 and 1.921 Å to produce a complex IM7. This process, again, is associated with a decrease in energy (−36.7 kJ mol^{-1}) but an increase in Gibbs free energy (13.5 kJ mol^{-1}) due to the decrease of entropy.

IM7 may isomerize into IM8 *via* another seven-member ring (C8-H19-O20-H18-O16- H12-N9) transition state TS4 with an energy barrier of 95.6 kJ mol^{-1}. In TS4, the two water molecules are located above the plane of the imidazole ring and H19 interacts strongly with the O20 atom of a water molecule that leads to the breaking of the C8-H19 bond. The H12 atom in another water molecule interacts strongly with the N9 atom and forms a N9-H12 bond. This is also a process of H exchange with the assistant of the two water molecules (*i.e.*, bonding H19 and releasing H12). The water molecule attaching H19 moves significantly toward H14 and S10 atoms and another water molecule attaching H12 also moves significantly toward H12 and H14 atoms to form the stable complex, IM8, a structure of four hydrogen bonds.

At the end of Fig. 3, the profile shows that the two water molecules may leave IM8 with an increase of the Gibbs free energy by 19.8 kJ mol^{-1} (or an internal energy by 70.1 kJ mol^{-1}) to produce the isolated **N(9)H**.

The rate-determining step in the pathway **P(2)** is the transition of IM5 to TS3 that has a relatively higher activation energy barrier of 202.5 kJ mol^{-1}. The barrier will be reduced to 177.8 kJ mol^{-1} by considering the long-range solvent effect, showing that the long-range solvent also has an important effect on the tautomerization reaction energies.

Table 4 Relative Gibbs free energies (ΔG in kJmol^{-1} at 298.15 K)[a] for the species of mono- and di-hydration reactions for **P(7)** and **P(8)** calculated with B3LYP/Aug-cc-pVTZ//B3LYP/6-311+G**

Mono-hydrated	ΔG[b]	Di-hydrated	ΔG[c]
N(7)H+H_2O	0.0 (0.0)	N(7)H+2H_2O	0.0 (0.0)
IM1	−14.2 (−7.9)	IM5	−7.8 (−18.3)
TS15	251.0 (199.9)	TS16	176.2 (94.5)
IM4	33.8 (13.5)	IM8	17.5 (4.2)
N(9)H+H_2O	37.3 (12.6)	N(9)H+2H_2O	37.3 (12.6)

[a] Energy in the parentheses is for the aqueous phase

[b] Relative Gibbs free energy with respect to **N(7)H+H_2O** for mono-hydration

[c] Relative Gibbs free energy with respect to **N(7)H+2H_2O** for di-hydration

Proton transfer via C8 carbene complexes in the imidazole ring

Pathway P(3) **P(3)** is the transfer *via* C8 carbene and is associated with one solvent molecule as shown in Fig. 4.

A water molecule is first combined with the isolated reactant **N(7)H** to produce an intermediate IM9 with the formation of two intermolecular hydrogen bonds. One of which is between N9 and H17 with a distance of 2.079 Å and the other is between H13 and O16 with 2.634 Å. In IM9, the O16 and H17 atoms of the water molecule are almost in the molecular plane of **N(7)H**. It is shown in Table 2 that IM9 has a small positive relative Gibbs free energy (9.6 kJ mol^{-1}) but has a negative relative energy (−13.3 kJ mol^{-1} at 0 K) as provided in Supplement 4 due to the decrease of entropy.

In the formation of TS5, the C8-H13 and O16-H17 bonds would be elongated by 0.343 Å and 0.315 Å, and the N9…H17 and O16…H13 bonds would be shortened by 0.835 Å and 1.417 Å with an energy barrier of 220.1 kJ mol^{-1} that has an almost planer five-member ring. The imaginary vibration shows that the TS proceeds a concerted double

Table 5 Relative Gibbs free energies (ΔG in kJmol^{-1} at 298.15 K)[a] for the species of mono- and di-hydration reactions *via* the O, S and N atoms of pyrimidine ring calculated with B3LYP/Aug-cc-pVTZ//B3LYP/6-311+G**

Mono-hydrated	ΔG_{gas}[a]	Di-hydrated	ΔG_{gas}[a]
N(7)H+ H_2O	0.0	N(7)H+ $2H_2O$	0.0
IM1	−14.2	TS43	61.9 (82.0) [47.4]
TS17	60.6 (74.8)[58.0]	IM68	42.5
IM26	43.7	IM69	65.2
IM27	75.6	TS44	129.6 (64.4) [33.2]
TS18	159.0 (83.4) [60.4]	IM70	59.3
IM28	74.8	IM71	79.1
IM29	78.8	TS45	149.4 (70.3) [42.3]
TS19	135.5 (56.7) [52.3]	IM72	74.5
IM30	68.0	IM73	74.6
IM31	76.5	TS46	149.2 (74.6) [35.6]
TS20	148.7 (72.2) [55.0]	IM74	112.1
IM32	109.5	IM75	84.3
IM33	79.9	TS47	153.2 (68.9) [45.2]
TS21	146.7 (66.8) [41.1]	IM76	113.7
IM34	115.4	IM77	82.7
IM35	97.6	TS48	135.2 (52.5) [37.0]
TS22	161.6 (64.0) [56.0]	IM78	45.9
IM36	55.4	IM79	77.0
IM37	91.6	TS49	132.3 (55.3) [30.6]
TS23	160.3 (68.7) [51.6]	IM80	45.1
IM38	56.8	IM81	5.9
IM39	4.8	TS50	100.6 (94.7) [61.1]
TS24	101.6 (96.8) [79.9]	IM82	68.4
IM40	68.2	IM83	44.5
IM41	53.0	TS51	120.0 (75.5) [47.7]
TS25	111.1 (58.1) [49.5]	IM84	81.8
IM42	72.1	IM85	57.3
TS26	173.1 (101.0) [67.8]	TS52	146.5(89.2) [43.1]
IM43	115.2	IM86	98.5
IM44	93.0	IM87	83.7
TS27	114.6 (21.6) [27.2]	TS53	122.5 (38.8) [28.9]
IM45	48.7	IM88	52.5
IM46	4.3	IM89	−1.3
TS28	119.7 (115.4) [74.6]	TS54	92.6 (93.9) [44.0]
IM47	76.1	IM90	54.1
IM48	67.3	IM91	57.9
TS29	102.6(35.3) [32.4]	TS55	103.8(45.9) [22.5]
IM49	61.6	IM92	62.5
IM50	101.5	IM93	105.0
TS30	181.2 (79.7) [77.7]	TS56	197.7 (92.7) [70.2]
IM51	129.8	IM94	135.3
TS31	98.5 (49.8) [37.1]	TS57	84.3(31.8) [34.9]
IM52	57.8	IM95	75.9
TS32	116.4 (58.6) [39.4]	IM96	55.8
IM53	44.9	TS58	113.1(57.3) [32.2]
IM54	58.1	IM97	33.3
TS34	105.4(47.3) [16.6]	IM98	56.8
IM55	29.4	TS59	109.4 (52.6) [−5.8][b]
IM56	76.8	IM99	71.8
TS35	105.4 (28.6) [16.3]	TS60	112.2 (40.4) [18.2]
IM57	67.8	IM100	84.7
IM58	54.7	IM101	52.4
TS36	114.1 (59.4) [39.1]	TS61	111.0(58.6) [25.6]
IM59	43.6	IM102	34.7
TS37	140.0 (72.2) [34.9]	IM103	70.0
IM60	78.0	TS62	151.1 (81.1) [18.1]
IM61	78.6	IM104	65.9
TS38	125.4 (46.8) [28.4]	IM105	68.8
IM62	39.9	TS63	113.2 (44.4) [14.2]
TS39	100.6 (32.6) [18.0]	IM106	34.3
IM63	70.4	IM107	73.4
IM64	49.8	TS64	106.1 (32.7) [27.4]
TS40	98.9 (49.1) [36.9]	IM108	62.1
IM65	71.4	IM109	55.8
TS41	147.4(76.0) [36.1]	TS65	95.7 (39.9) [33.6]
IM66	87.1	IM110	75.9
IM67	90.3	IM111	72.9
TS42	136.6 (46.3) [37.6]	TS66	159.3 (86.4) [19.6]
		IM112	73.9
		IM113	96.6
		TS67	125.7 (29.1) [33.5]
		IM114	82.3

[a] Relative Gibbs free energies of all mono- and di-hydrated complexes are given relative to **N(7)H+H_2O** of **P(1)** and **N(7)H+$2H_2O$** of **P(2)**, respectively. Free energy barriers of reactions are given in parenthesis and the results in PCM model are given in the middle bracket

[b] The negative energy barrier, −5.8 kJmol^{-1} should be from the computational errors since the PCM model does not re-optimize the structures of the molecules

proton transfer where the hydrogen H17 in the water transfers onto the N9 atom and the atom H13 attaching C8 of the imidazole ring shifts onto the O16 atom of the water molecule. It is shown that this transition has a larger activation energy. However, this barrier is lowered by 86.1 kJ mol^{-1} from that (306.2 kJ mol^{-1}) without the existence of the water molecule obtained previously [1], implying that one water molecule would dramatically catalyze the reaction in this pathway (pathway **P(3)**), but it is still less feasible due to the high barrier of 220.1 kJ mol^{-1}.

Intermediate IM10 may be produced following TS5 with an energy release of 98.2 kJ mol^{-1}. IM10 is a complex of a

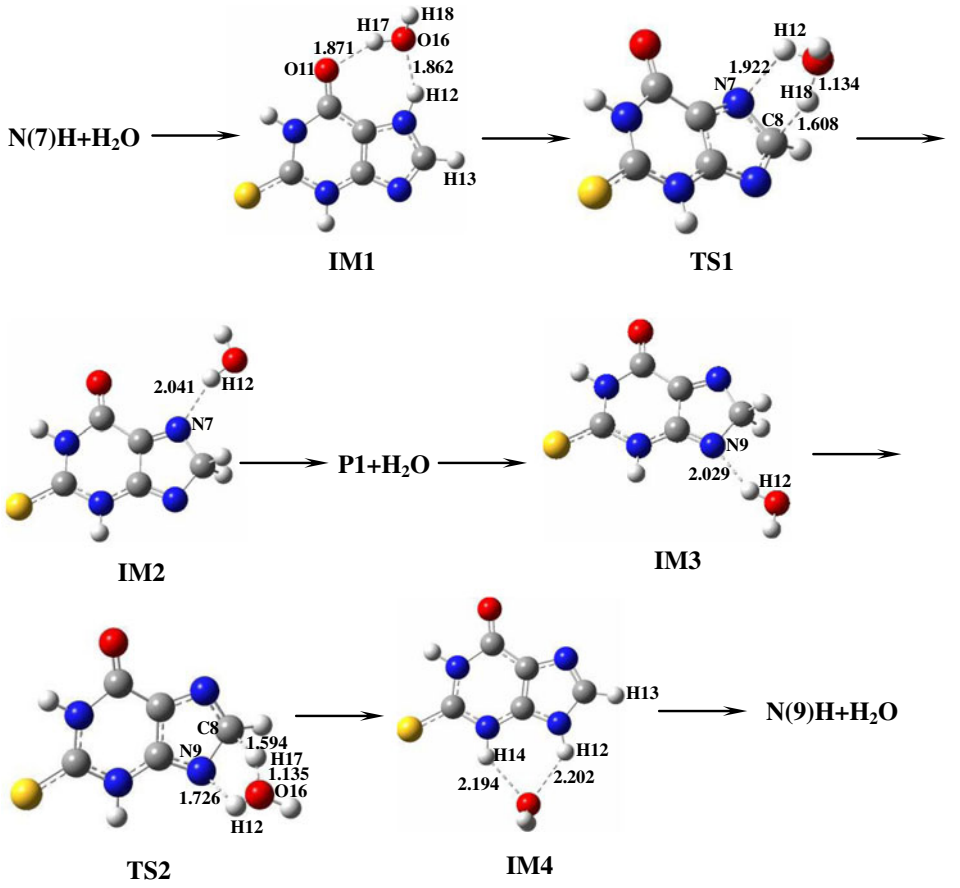

(a) structure

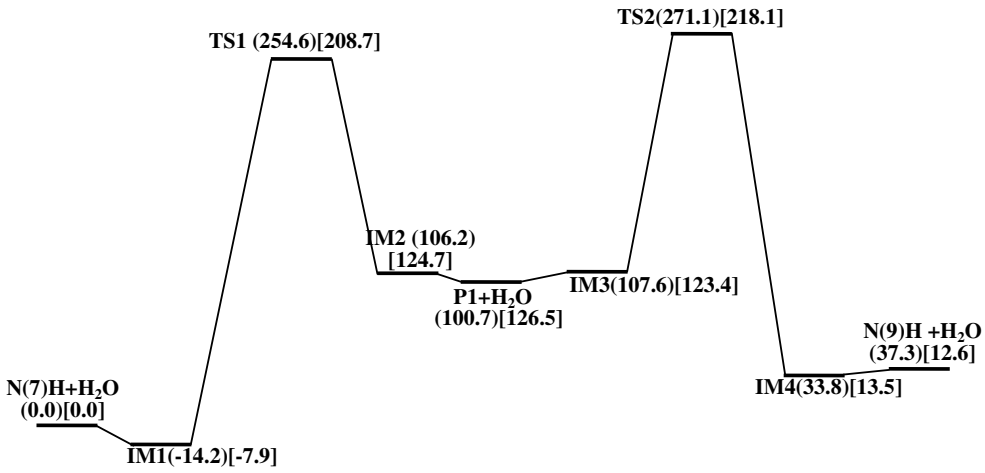

(b) energy profile

Fig. 2 Reaction pathway **P(1)** for one water molecule assisted proton transfer tautomerization processes of 2-thioxanthine *via* tetrahedral C8 complexes. Energy or energy barrier is in kJ mol^{-1} and is the Gibbs free energy at 298.15 K obtained with B3LYP/aug-cc-pVTZ// B3LYP/6-311+G**. The energy in the parentheses is for the microsolvent model and that in the square brackets is for the aqueous phase

water molecule and an unstable tautomer of 2TX that is 133.1 kJ mol^{-1} higher in energy than the reactant N(7)H.

The water molecule would possibly leave the complex to produce a tautomer P2 by absorbing a very small positive (1.6 kJ mol^{-1}) Gibbs free energy. This process is associated with a thermodynamic energy (at 0 K) increase of 27.4 kJ mol^{-1} where the dissociation of the water molecule is a process of increasing entropy that resulted in a decrease of the Gibbs free energy.

Further tautomerization is proceeded that a water molecule may again interact with P2 and form two hydrogen bonds between C8…H13 and H12…O16 (with the distances of 2.152 and 2.204 Å, respectively) to produce a complex IM11. This is associated with a decrease in energy

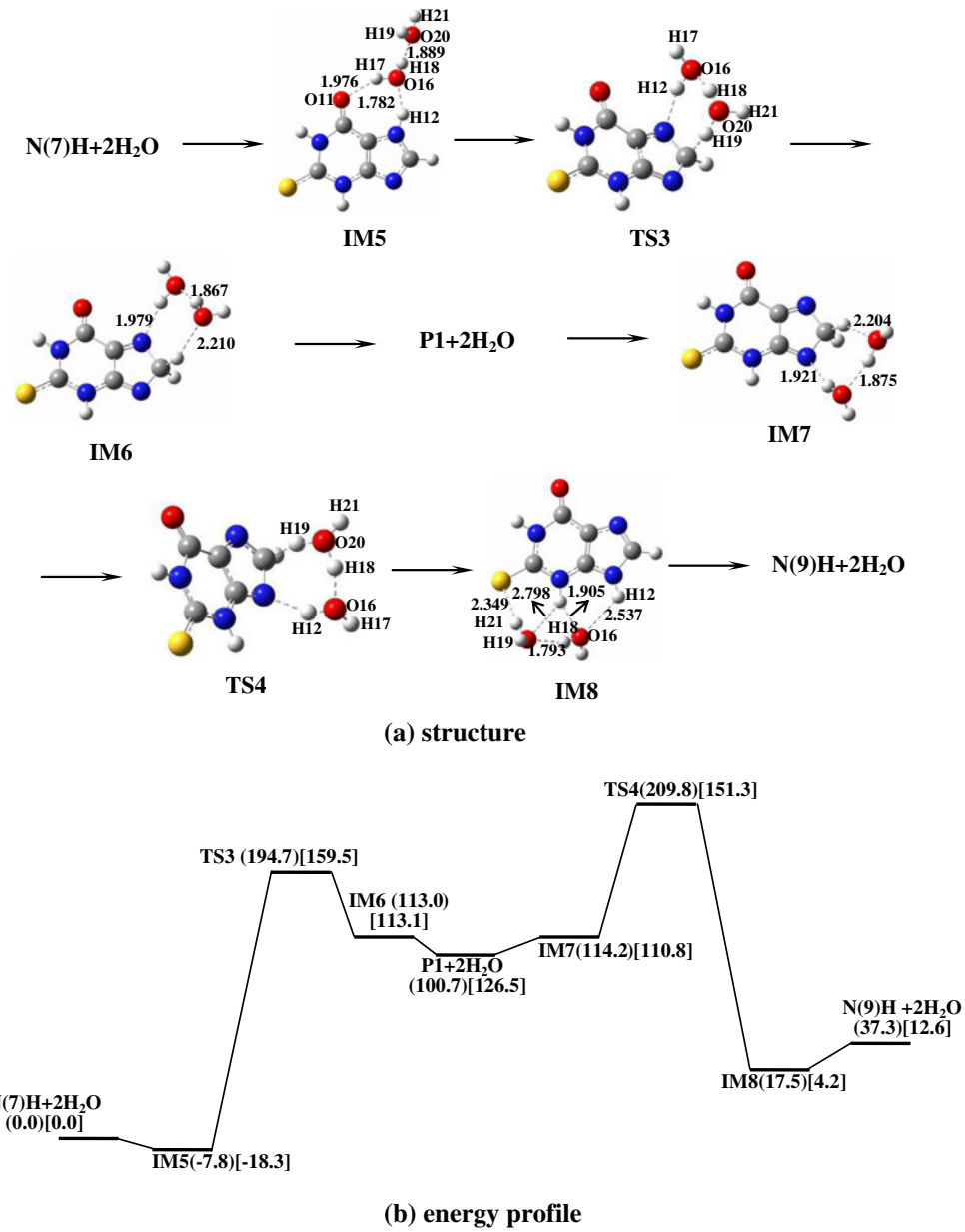

Fig. 3 Reaction pathway **P(2)** for two water molecules assisted proton transfer tautomerization processes of 2-thioxanthine *via* tetrahedral C8 complexes. Energy or energy barrier is in kJ mol^{-1} and is the Gibbs free energy at 298.15 K obtained with B3LYP/aug-cc-pVTZ//B3LYP/6-311+G**. The energy in the parentheses is for the microsolvent model and that in the square brackets is for the aqueous phase

(−21.2 kJ mol^{-1}) but slight increase in Gibbs free energy (4.5 kJ mol^{-1}).

IM11 may isomerize into IM12 *via* another five-member ring (C8-N7-H12-O16-H13) transition state TS6 with a barrier of 114.4 kJ mol^{-1} in which the water molecule is almost in the plane of the imidazole ring except for H18. The N7-H12 and O16-H13 bonds are elongated by 0.227 Å and 0.275 Å while the C8…H13 and O16…H12 bonds are shortened by 0.766 Å and 0.911 Å, respectively. The normal mode of the imaginary vibration indicates that the dissociation of TS6 follows a concerted double proton transferring mechanism where the atom H13 in the water transfers onto C8 atom and the H12 attaching N7 of the imidazole ring shifts onto O16 of the water. This is also a H exchange with the assistance of the water molecule (*i.e.*, bonding H13 and releasing H12). In this transition, the N7-H12 and O16-H13 bonds are broken and the bond angle of C8- N7-H12 is reduced largely by 22.3°. The formation of IM12, a complex of a water molecule and the product N(9)H, is associated with an energy release of 183.5 kJ mol^{-1}.

Finally, the water molecule will easily leave IM12 with a small decrease of the Gibbs free energy of 2.6 kJ mol^{-1} (or an internal energy increase of 17.9 kJ mol^{-1}) and the isolated **N(9)H** tautomer is produced.

These results indicate that the rate-determining step of the pathway **P(3)** is the transition of IM9 to TS5 that has a higher activation energy barrier of 220.1 kJ mol^{-1}. After considering the long-range solvent effect using the PCM model, this value is slightly reduced to 208.5 kJ mol^{-1}.

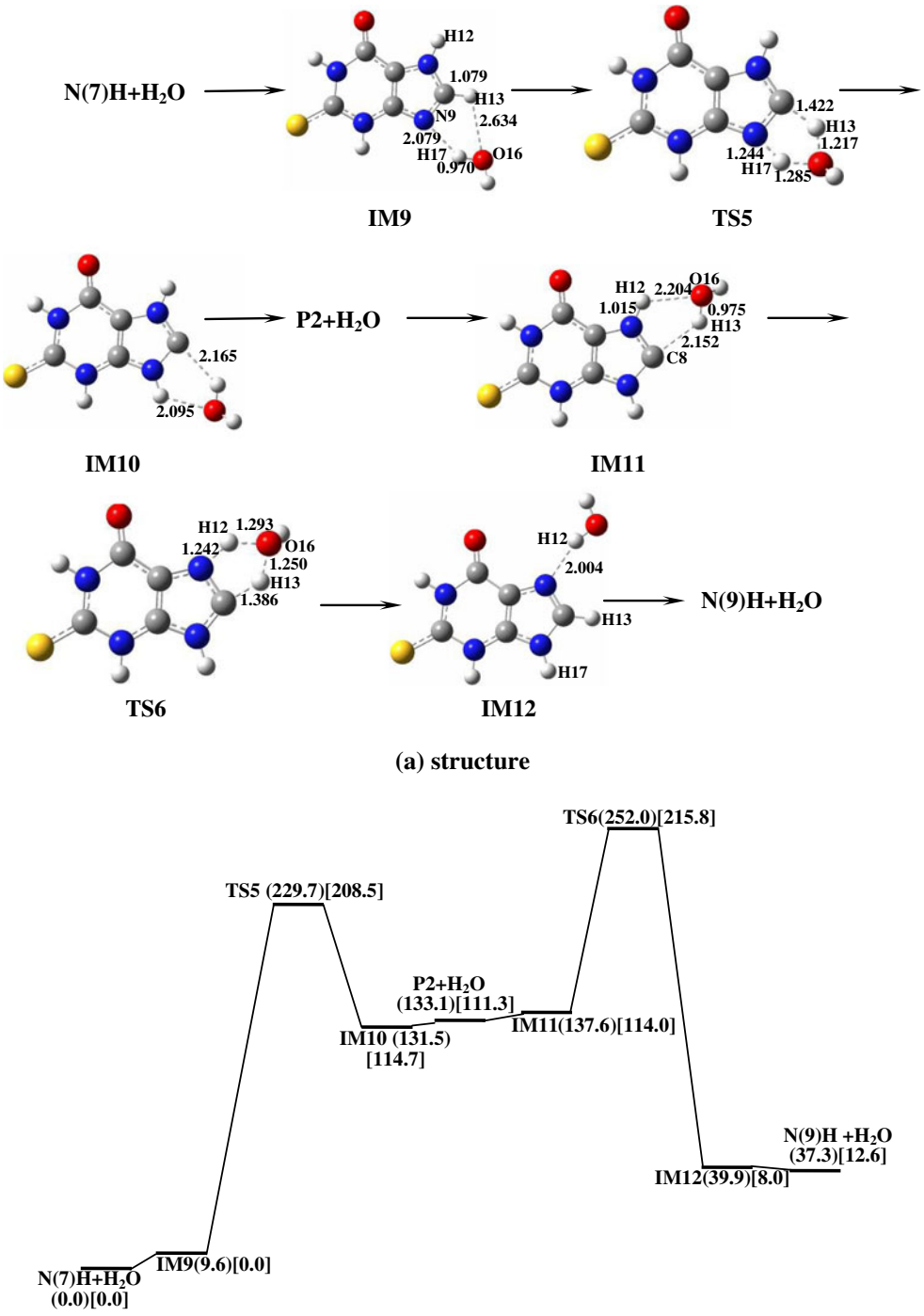

Fig. 4 Reaction pathway **P(3)** for one water molecule assisted proton transfer tautomerization processes of 2-thioxanthine *via* carbene C8 complexes. Energy or energy barrier is in kJ mol^{-1} and is the Gibbs free energy at 298.15 K obtained with B3LYP/aug-cc-pVTZ//B3LYP/6-311+G**. The energy in the parenthesis is for the microsolvent model and that in the bracket is for the aqueous phase

In this pathway, the relative Gibbs free energies of the complexes IM9 and IM12 are 23.8 and 54.1 kJ mol^{-1} with respective to IM1 (Supplement 5) predicting that the relative concentrations of IM9 and IM12 are 6.8×10^{-5} and 3.3×10^{-10} at 298.15 K. Although the relative concentrations of those may be increased into 4.1×10^{-2} and 1.6×10^{-3} in the aqueous phase with respective to IM1, only IM9 can be observable that has a relative concentration larger than 1 ppm with respect to the most stable IM21 (Supplement 5).

At this point, the importance of the long range solvent effects reminds us of the choice of the computational methods. As an examination for the barrier of TS6, the PCM model resulted in a smaller value of 101.8 kJ mol^{-1} compared with that 114.4 kJ mol^{-1} without the effects. The CPCM model [40, 41], interestingly, reproduced exactly the same result as PCM while a recently proposed SMD model [42] resulted in a slightly larger value of 105.6 kJ mol^{-1} that has a deviation of

3.8 kJ mol^{-1} (or less than 1 kcal mol^{-1}) from PCM. Therefore, further study will employ only the PCM model.

Pathway P(4) **P(4)** is the pathway similar to **P(3)** but is associated with two water molecules as shown in Fig. 5.

IM13 is the complex of two water molecules and the isolated reactant **N(7)H** that has three intermolecular hydrogen bonds between N9 and H19 in 1.942 Å, O18 and H17 in 2.634 Å and between O16 and H13 in 2.136 Å. The O16, H17, O18 and H19 atoms of the two water molecules are almost co-planer with **N(7)H**. Data in Table 2 show that IM13 has a small positive relative Gibbs free energy (9.8 kJ mol^{-1}) with respect to **N(7)H+2H$_2$O** while those in Supplement 6 show that IM13 has a negative relative energy (−40.7 kJ mol^{-1}), implying a significant decrease of entropy.

The C8-H13, O16-H17 and O18-H19 bonds in IM13 may be elongated by 0.154 Å, 0.429 Å and 0.529 Å, and the O16…H13, O18…H17 and N9…H19 bonds may be shortened by 0.778 Å, 0.772 Å and 0.847 Å, respectively, to produce an almost planer seven-member ring transition state TS7 with an energy barrier of 159.7 kJ mol^{-1}. This process is a concerted triple proton transfer as shown by the normal mode of the imaginary vibration that the hydrogen atom H19 in one water molecule transfers onto the N9 atom and the hydrogen atom H13 attaching C8 of the imidazole ring shifts onto the O16 atom of the water molecule. The activation energy is 60.4 kJ mol^{-1} lower than that (220.1 kJ mol^{-1}) in pathway **P(3)**, implying that two water molecules

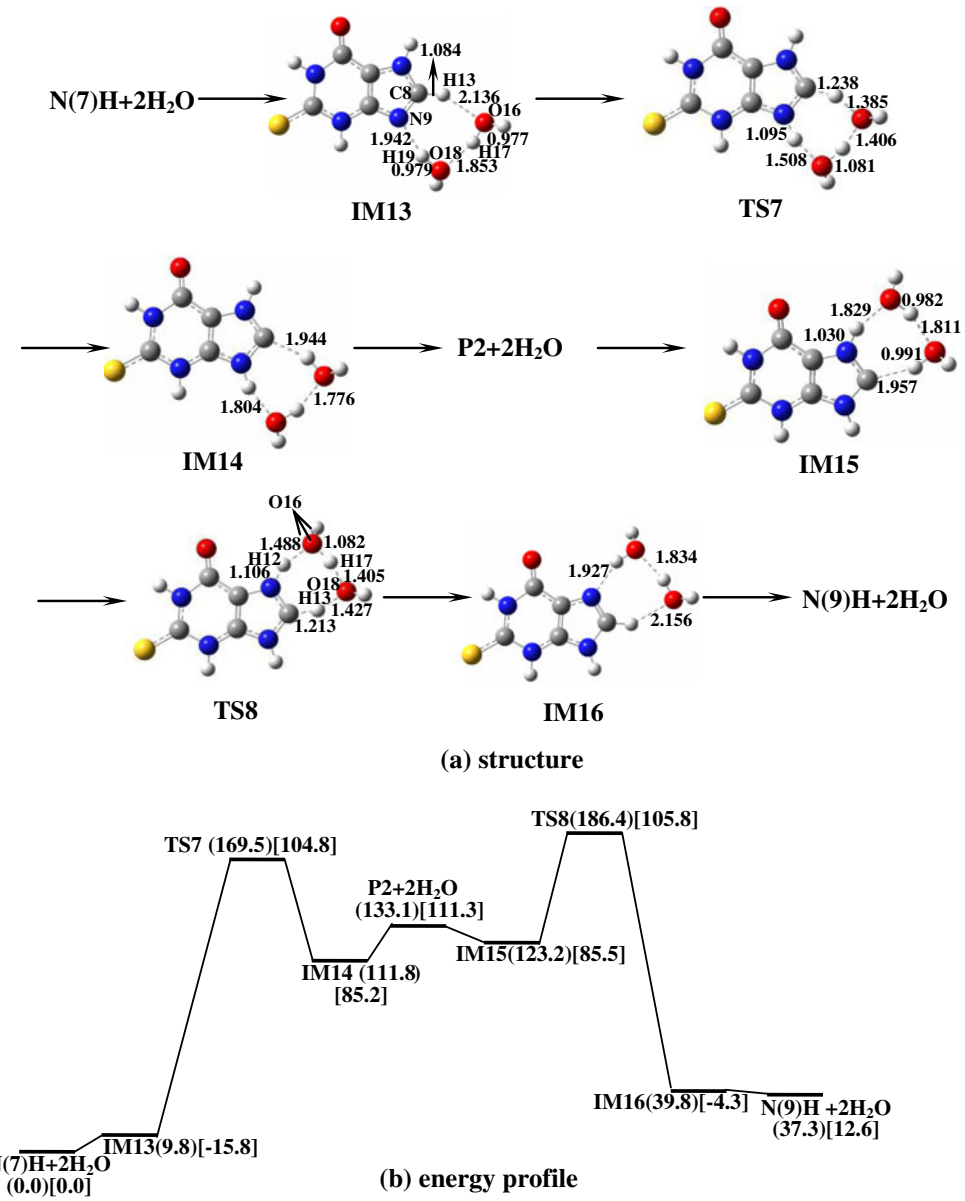

Fig. 5 Reaction pathway **P(4)** for two water molecule assisted proton transfer tautomerization processes of 2-thioxanthine *via* carbene C8 complexes. Energy or energy barrier is in kJ mol^{-1} and is the Gibbs free energy at 298.15 K obtained with B3LYP/aug-cc-pVTZ//B3LYP/6-311+G**. The energy in the parenthesis is for the microsolvent model and that in the bracket is for the aqueous phase

dramatically decreased the ring tension (*i.e.*, from five-member to seven-member) and would catalyze the reaction. After TS7, intermediate IM14 may be produced with an energy release of 34.3 kJ mol^{-1}. The two water molecules in IM14 would leave the complex to produce a tautomer P2 by absorbing 21.3 kJ mol^{-1} of the Gibbs free energy or 74.1 kJ mol^{-1} (at 0 K) of the thermodynamic energy.

Two water molecules may again interact with P2 at other sites and produce three hydrogen bonds between C8 and H13, O18 and H17, and O16 and H12 with the respective distances of 1.957, 1.811 and 1.829 Å to produce a complex IM15. This, again, is associated with a significant decrease of energy (−63.0 kJ mol^{-1}) and slight decrease of Gibbs free energy (−9.9 kJ mol^{-1}).

IM15 may isomerize into IM16 *via* another seven-member ring (C8-N7-H12-O16-H17-O18-H13) transition state TS8 with an energy barrier of 63.2 kJ mol^{-1}, where the two water molecules are almost in the plane of the imidazole ring. The N7-H12, O16-H17 and H13-O18 bonds are elongated by 0.076 Å, 0.100 Å and 0.436 Å, and the C8-H13, O18-H17 and O16-H12 bonds are shortened by 0.744 Å, 0.406 Å and 0.341 Å, respectively. This is a concerted triple proton transfer-ring reaction where the H13 atom in one water molecule transfers onto C8 atom and the H12 atom attaching N7 of the imidazole ring shifts onto O16 of another water molecule. This is also a process of H exchange with the assistant of the two water molecules (*i.e.*, bonding H13 and releasing H12). TS8 may easily transform into intermediate IM16, a complex of two water molecules and the product **N(9)H**, with an energy release of 121.5 kJ mol^{-1}. The water molecules will spontaneously leave the complex IM16 due to a decrease of 2.5 kJ mol^{-1} of the Gibbs free energy (that has an increase of 48.0 kJ mol^{-1} of the thermodynamic energy) to produce the **N(9)H** tautomer.

These results indicate that the rate-determining step of the pathway **P(4)** is the transition of IM13 into TS7 that has an energy barrier of 159.7 kJ mol^{-1}. In the long-range water solvent, this data is further reduced to 120.6 kJ mol^{-1}, a value that is much lower than those in the previous pathways.

Proton transfer via bridge carbon C4 and C5 between the pyrimidine and the imidazole rings

Pathway P(5) **P(5)** is the transfer associated with one water molecule as shown in Fig. 6.

The first step in **P(5)** is the same as that in pathway **P(1)** and also produces IM1. The next step is that the water molecule moves onto the imidazole ring above C5-N7 bond from the purine ring plane and forms a five-member ring transition state TS9 with an energy barrier of 251.7 kJ mol^{-1}. The imaginary vibration of TS9 also corresponds to a concerted double proton transferring where H17 in the water molecule transfers onto C5 and H12 attaching N7 of the imidazole ring shifts onto O16 of the water molecule. Obviously, this barrier is even higher than that (224.9 kJ mol^{-1}) without the existence of the water molecule obtained previously [1], implying that pathway **P(5)** is less feasible.

Intermediate IM17 might be produced following TS9 with an energy release of 93.9 kJ mol^{-1} and the C5 atom in IM17 is saturated with four sp^3-type bonds (*i.e.*, two C-C, one C-N and one C-H) associated with the formation of two hydrogen bonds between N7-H12 and O16-H17 with the distances of 2.078 and 2.583 Å. These bonds would lead to the breaking of the conjugated bond between the pyrimidine and imidazole rings. IM17 is also a complex of a water molecule and an unstable tautomer P3 of 2TX that is 113.8 kJ mol^{-1} higher in energy than the reactants. In IM17, the water molecule would spontaneously leave the complex to produce the tautomer P3 due to a negative (−7.8 kJ mol^{-1}) Gibbs free energy change.

P3 may further interact with a water molecule to produce a complex IM18 with the formation of a hydrogen bond between O16 and H17 (at a distance of 2.140 Å). This process is associated with a decrease in energy (−11.2 kJ mol^{-1}) but slight increase in Gibbs free energy (8.6 kJ mol^{-1}) due to entropy decreasing. IM18 may isomerize into IM19 *via* a transition state TS10 with an energy barrier of 135.7 kJ mol^{-1}. In TS10, the water molecule is located above the shifting hydrogen H17 without participating in the proton transfer. This is thus a process of intramolecular proton transfer with the existence of one water molecule. Following this step, the water molecule will easily leave IM19 with a decrease of the Gibbs free energy by 10.3 kJ mol^{-1} and the tautomer P4 is produced.

P4 may combine a water molecule to form a complex IM20 with the formation of three hydrogen bonds. This is associated with a decrease in energy (−15.1 kJ mol^{-1}) but with an increase in Gibbs free energy (10.0 kJ mol^{-1}) due to entropy decreasing. IM20 may isomerize into IM4 *via* a transition state TS11 with an energy barrier of 106.1 kJ mol^{-1}. In TS11, the water molecule is also located above the shifting hydrogen H17 without participating in the proton transfer corresponding to an intramolecular proton transfer. Finally, the water molecule will be dissociated from IM4 with a small decrease of the Gibbs free energy of 3.5 kJ mol^{-1} and the tautomer N(9)H is produced.

These results indicate that the rate-determining step of the pathway **P(5)** is the transition of IM1 to TS9 that has a higher activation energy barrier of 251.7 kJ mol^{-1}. After considering the long-range solvent effect using the PCM model, this barrier is reduced to 212.4 kJ mol^{-1}, showing that the long-range solvent effect is important in the tautomerization reactions.

Pathway P(6) **P(6)** is similar to **P(5)** but associated with two water molecules as shown in Fig. 7.

Combination of two water molecules and the isolated reactant **N(7)H** will produce intermediate IM21 with the formation of three planer intermolecular hydrogen bonds

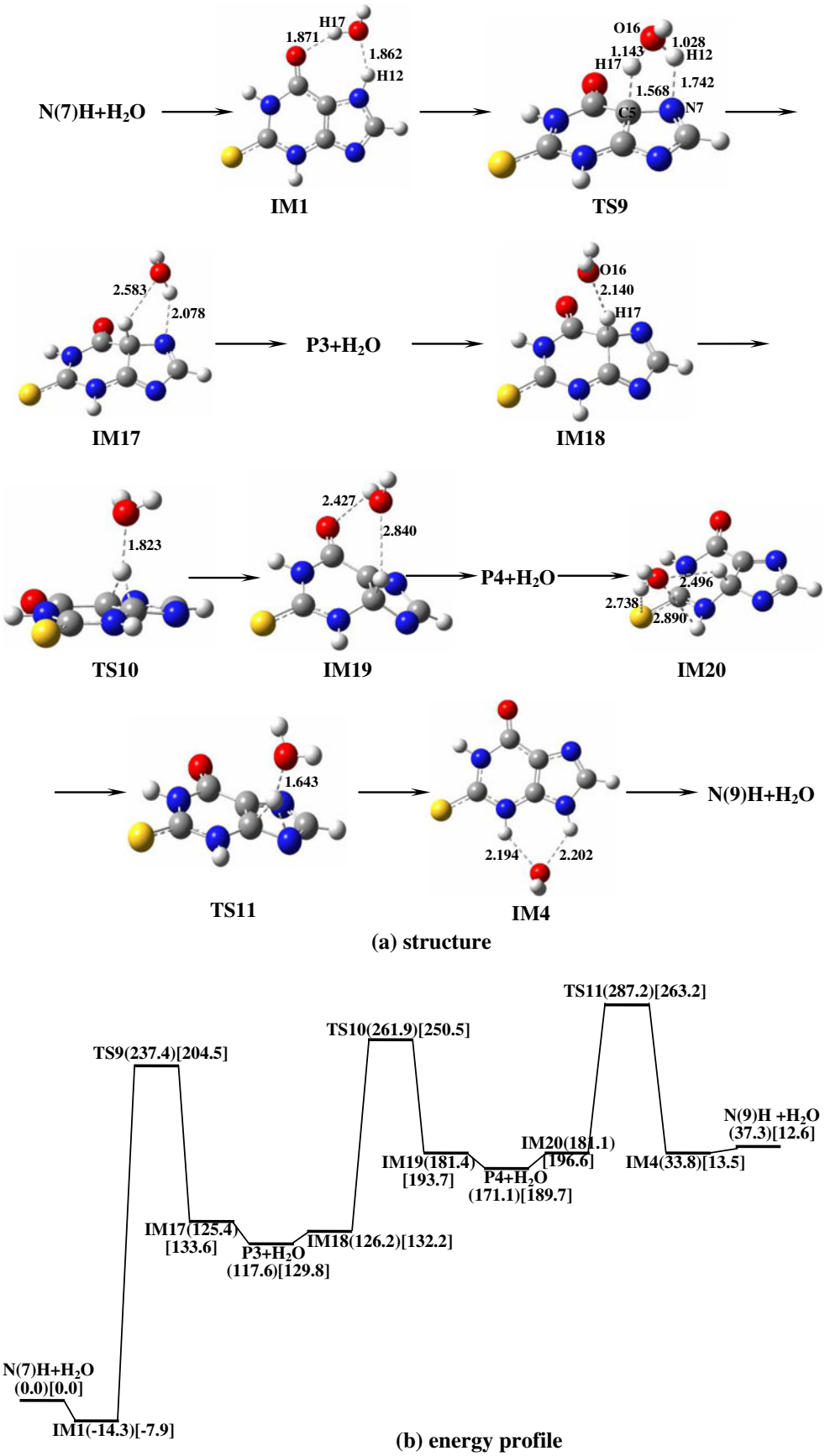

Fig. 6 Reaction pathway **P(5)** for one water molecule assisted proton transfer tautomerization processes of 2-thioxanthine *via* bridge carbon C4 and C5. Energy or energy barrier is in kJ mol^{-1} and is the Gibbs free energy at 298.15 K obtained with B3LYP/aug-cc-pVTZ// B3LYP/6-311+G**. The energy in the parenthesis is for the microsolvent model and that in the bracket is for the aqueous phase

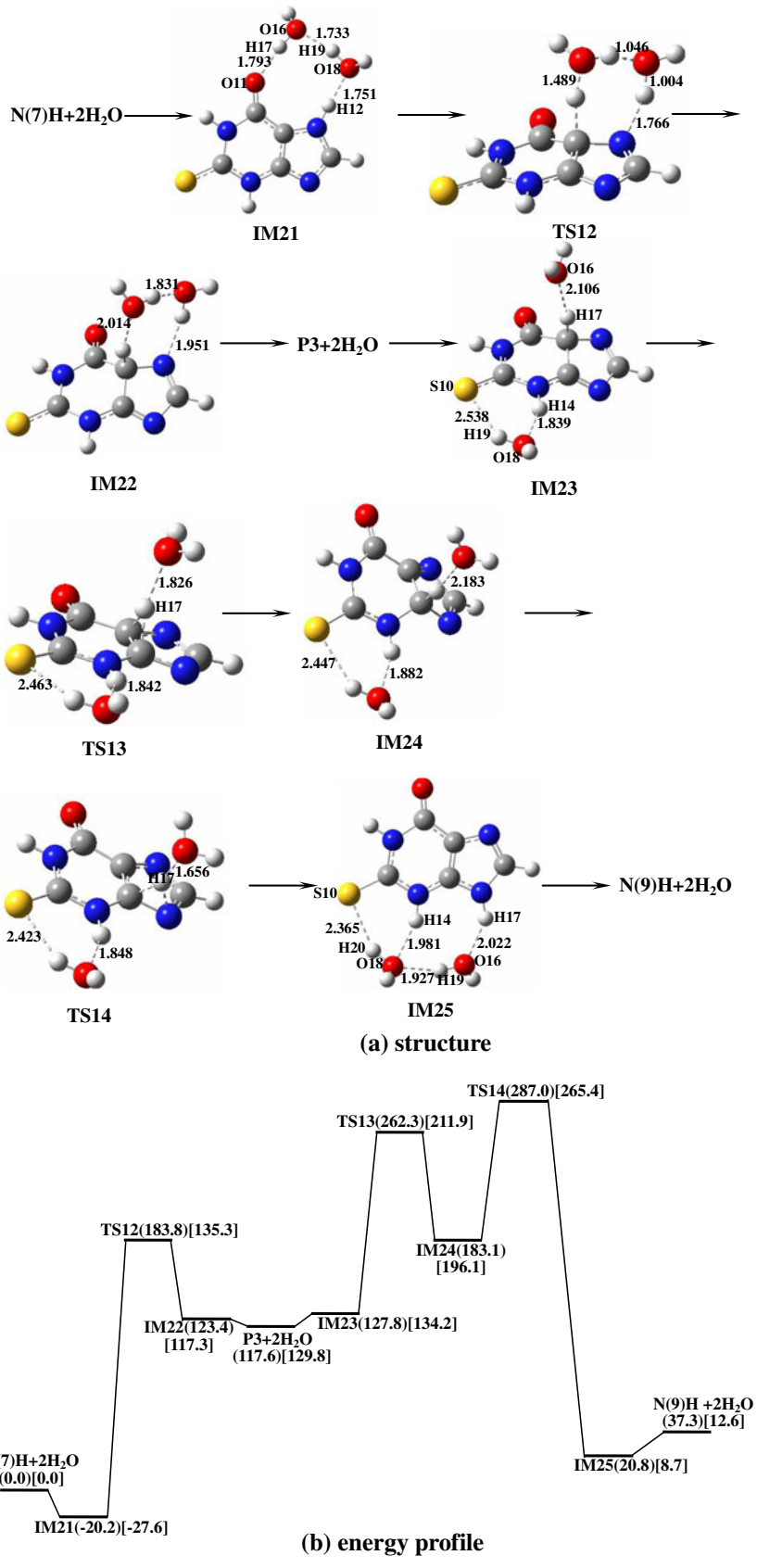

Fig. 7 Reaction pathway **P(6)** for two water molecule assisted proton transfer tautomerization processes of 2-thioxanthine *via* bridge carbon C4 and C5. Energy or energy barrier is in kJ mol^{-1} and is the Gibbs free energy at 298.15 K obtained with B3LYP/aug-cc-pVTZ// B3LYP/6-311+G**. The energy in the parenthesis is for the microsolvent model and that in the bracket is for the aqueous phase

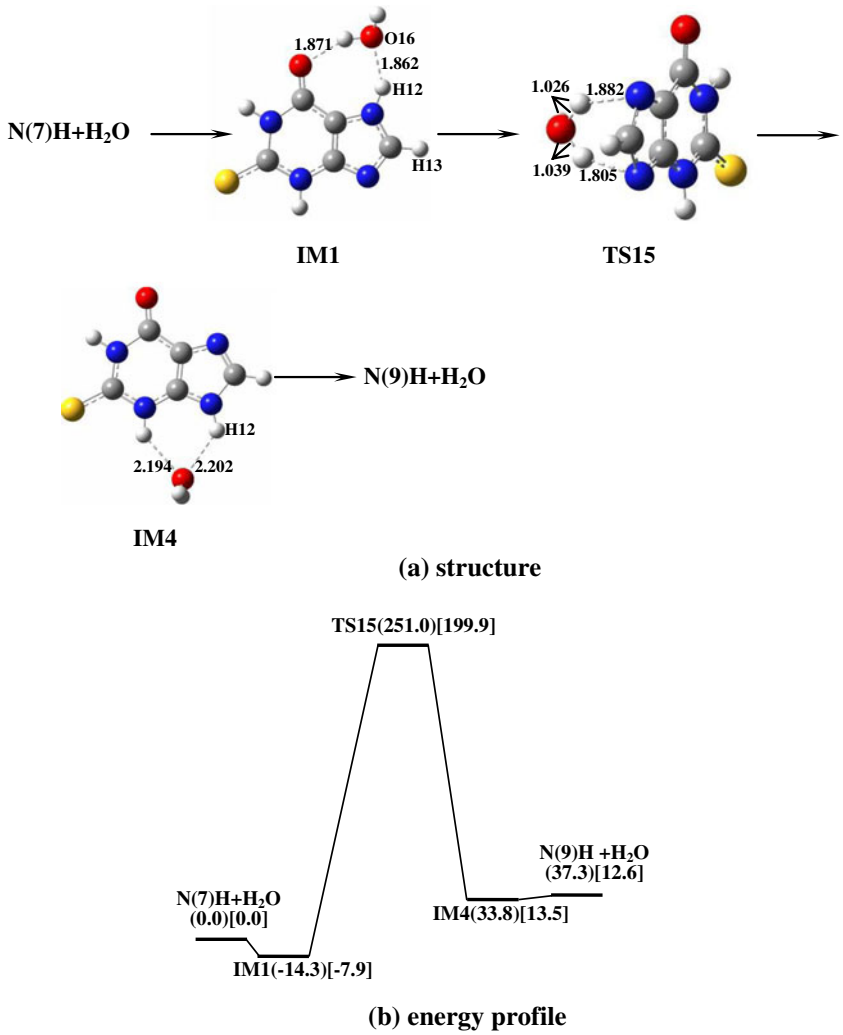

Fig. 8 Reaction pathway **P(7)** for direct proton transfer with one water molecule catalysis of 2-thioxanthine. Energy or energy barrier is in kJ mol^{-1} and is the Gibbs free energy at 298.15 K obtained with B3LYP/aug-cc-pVTZ//B3LYP/6-311+G**. The energy in the parenthesis is for the microsolvent model and that in the bracket is for the aqueous phase

O11…H17 with a distance of 1.793 Å, O16…H19 with 1.733 Å and O18…H12 with 1.751 Å. In IM21, the O16, H17, O18 and H19 atoms of the water molecules are almost in the molecular plane of **N(7)H**. The two water molecules may move onto the imidazole ring above C5-N7 bond from the purine ring plane and form a seven-member ring transition state TS12 with an energy barrier of 204.0 kJ mol^{-1} that follows a concerted triple proton transferring mechanism. In which, the hydrogen H17 in one water molecule transfers onto C5 and the atom H12 attaching N7 in the imidazole ring shifts onto O18 of another water molecule. The activation energy 204.0 kJ mol^{-1} is lower than either the value 224.9 kJ mol^{-1} without the existence of the water molecule [1] or the barrier 251.7 kJ mol^{-1} with one water in pathway **P(5)**. Therefore, two water molecules are able to catalyze the tautomerization but pathway **P(6)** should also be less feasible due to the higher barrier.

IM22 would be produced following TS12 with an energy release of 42.5 kJ mol^{-1}. In this process, the C5 atom in IM22 is also saturated with four sp^3-type bonds (*i.e.*, two C-C, one C-N and one C-H single bonds) associated with the formation of hydrogen bonds between N7…H12, O18…H19 and O16…H17 with the distances of 1.951, 1.831 and 2.014 Å that leads to the breaking of the conjugation bond between the pyrimidine and imidazole rings. The water molecules would spontaneously leave IM22 to produce the tautomer P3 due to a negative (−5.8 kJ mol^{-1}) Gibbs free energy change although the thermodynamic energy (at 0 K) increases by 45.2 kJ mol^{-1}.

P3 could also interact with other water molecules. In our case, a hydrogen bond between O16 and H17 and two hydrogen bonds between O18…H14 and H19…S10 are formed that leads to the production of complex IM23. This process is associated with a decrease in energy (−35.4 kJ mol^{-1}) but with an increase in Gibbs free energy (10.2 kJ mol^{-1}) due to entropy decreasing.

IM23 may isomerize into IM24 *via* transition state TS13 with an energy barrier of 134.5 kJ mol^{-1}. In TS13, one water molecule is located above the shifting hydrogen H17 but it will not participate in the proton transfer reaction. This reaction is identified as an intramolecular proton transfer with the existence of two water molecules. Further

tautomerization of IM24 is proceeded where H17 shifts onto N9 *via* a transition state TS14 with an energy barrier of 103.9 kJ mol^{-1}. Similar to that in TS13, a water molecule in TS14 is located above the shifting hydrogen H17 but will not participate in the proton transfer reaction. After carrying out IRC analyses starting from TS14, complex IM25 is found, in which four hydrogen bonds between O16…H17, O18…H19, O18…H14 and S10…H20 (with the distances of 2.022, 1.927, 1.981 and 2.365 Å) are formed. Finally, the water molecules would leave the complex with a small increase of the Gibbs free energy by 16.5 kJ mol^{-1} (or an increase of internal energy by 69.3 kJ mol^{-1}) and the tautomer **N(9)H** is produced.

By considering the long-range solvent effect using the PCM model, the highest barrier (204.0 kJ mol^{-1}) in the transition of IM21 to TS12 is reduced to 162.9 kJ mol^{-1}, showing that the long-range solvent effect is important in this pathway.

As examined so far (and also for all the discussions over the paper), we found that the intermediates in the two water microsolvent models are relatively lower in energy than those in the one water models, and IM21 [**N(7)H**-$2H_2O$] is the most stable complex either with or without the long-range solvent. The data in Supplement 5 also show that the application of the long-range solvent model will increase the predicted concentration of the respective species. In the present pathway **P(6)**, for example, the relative concentrations of IM5, IM8, IM13 and IM25 are 6.7×10^{-3}, 2.5×10^{-7}, 5.5×10^{-6} and 6.6×10^{-8} without the long-range solvent but are increased into 2.0×10^{-2}, 2.7×10^{-6}, 8.6×10^{-3} and 4.4×10^{-7} in the aqueous phase. This also predicts that IM5, IM8 and IM13 are possible to be observed in co-existence with IM21 since their relative concentrations are larger than 1 ppm. Interestingly, IM16 has a very low concentration of 3.1×10^{-11} but increases significantly into 8.3×10^{-5} (an observable value) in the aqueous phase.

Direct proton transfer with one or two water molecules catalysis

Pathway P(7) **P(7)** is a direct process for N(7)H→N(9)H transition in the existence of one water molecule as shown in Fig. 8.

This path has the same reactant and product complexes IM1 and IM4 as in pathway **P(1)**. The major difference is that the shifting proton can directly move between N7 and N9 atoms which does not need to transfer *via* C8 atom (as in **P(1)**, **P(2)**, **P(3)** and **P(4)**) or C4 and C5 atoms (as in **P(5)** and **P(6)**). Figure 8 shows a double proton transfer mechanism where the water molecule above the imidazole ring acts as a bridge linking the two protons. The IRC analysis reveals that the reactant IM1 and the product IM4 are linked with a single transition state TS15 with a higher barrier of 265.2 kJ mol^{-1} (Table 4). However, this barrier is decreased to 207.8 kJ mol^{-1} by involving the water solvent, implying that the solvent effect is preferred to facilitate the proton transfer.

Pathway P(8) **P(8)** is associated with two water molecules as shown in Fig. 9.

This path has the same reactant complex (IM5) and product complex (IM8) as in **P(2)**. Compared with **P(7)**, this path follows a triple proton transfer mechanism in which the water molecules above the imidazole ring also act as a bridge role between N7 and N9 atoms. The IRC analysis shows that the reactant IM5 and the product IM8 are linked with transition state TS16 with a much lower barrier of 184.0 kJ mol^{-1} (lowered by 81.2 kJ mol^{-1} than 265.2 kJ mol^{-1} of **P(7)** as shown in Table 4). By involving the water solvent, the value is further decreased to 112.8 kJ mol^{-1} and is the lowest barrier found so far. This value is also adequate for a reaction to have a reasonable reaction rate even at room temperature.

Proton transfer reactions via the O, S and N atoms in the pyrimidine ring facilitated by one water molecule

The proton transfers are also possible *via* the O, S and N atoms of the pyrimidine ring.

Similarly, the reactions with the existence of one or two water molecules are examined. The optimized geometrical structures and parameters for the one water assistant species of 43 stable complexes and 25 transition states are summarized in Fig. 10. The isolated intermediates (P5-P19) are shown in Fig. 11. The energy profiles of the one water assistant reaction pathways are illustrated in Fig. 12 drawn in two panels where panel (a) is for mono-hydrated N(7)H to mono-hydrated P7 or P10 and panel (b) is continued for mono-hydrated P7 to the product N(9)H.

For the reaction positions started at hydrogen atom H12, H14 or H15 (shown, *e.g.*, in Fig. 10), complex IM1, IM39 or IM46 is first formed (Fig. 12). Further intermediate IM26, IM40 and IM47 can be formed *via* the respective TS17, TS24 or TS28 with the free energy barrier of 74.8, 96.8 and 115.4 kJ mol^{-1}. However, all the barriers have a slightly smaller value, 58.0, 79.9 and 74.6 kJ mol^{-1}, in the continuum solvent PCM model, showing that the continuum solvent effect is considerable.

In the next steps, the water molecule may dissociate and produce an isolated P5, P11 or P13 tautomer with an increase of the Gibbs free energy at most by 32.5 kJ mol^{-1} in IM26 to P5+H_2O transition. And then, a water molecule can combine onto the hydrogen atom H14 or H15 of P5 and form complex IM27 or IM31 with the negligible energy

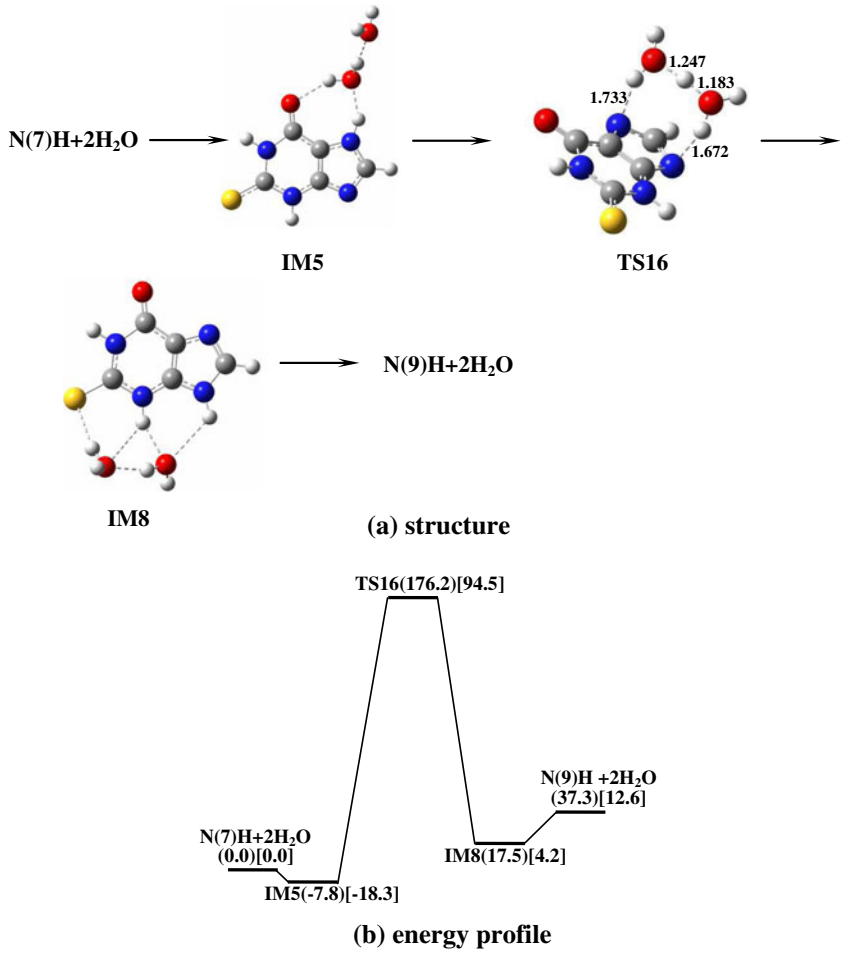

Fig. 9 Reaction pathway **P(8)** for direct proton transfer with two water molecule catalysis of 2-thioxanthine. Energy or energy barrier is in kJ mol^{-1} and is the Gibbs free energy at 298.15 K obtained with B3LYP/aug-cc-pVTZ//B3LYP/6-311+G**. The energy in the parenthesis is for the microsolvent model and that in the bracket is for the aqueous phase

change of −0.6 or 0.3 kJ mol^{-1}. Similarly, a water molecule may combine onto H12 or H14 of P11, or H12 or H15 of P13 and form complex IM41, IM42, IM48 or IM50 with a small energy change of −16.0, 3.1, −27.4 or 6.8 kJ mol^{-1}. These six complexes may, respectively, transfer into IM28, IM32, IM33, IM43, IM49 and IM51 *via* TS18, TS20, TS25, TS26, TS29 and TS30 with the free energy barriers of 83.4, 72.2, 58.1, 101.0, 35.3 and 79.7 kJ mol^{-1}. These values may be reduced to 60.4, 55.0, 49.5, 67.8, 32.4 and 77.7 kJ mol^{-1} in the PCM model, revealing, again, the considerable effect of the long-range solvent. The intermediates will also dissociate the water molecule to produce isolated tautomer P6, P8 or P12 with very small energy changes except IM33 that will directly isomerize into IM34 by the O-H bond rotation *via* TS21 with a barrier of 66.8 kJ mol^{-1}. In the next steps, a water molecule will recombine the H atom at another position of P6, P8 or P12 and form complexes IM29, IM37 and IM44 with the release of the Gibbs energies of 4.7, 11.4 and 35.1 kJ mol^{-1}. These intermediates will further transfer into P7 associated with the transition states TS19, TS23 and TS27 with the barriers of 56.7, 68.7 and 21.6 kJ mol^{-1}. The values are reduced to 52.3 and 51.6 kJ mol^{-1} for TS19 and TS23 in the PCM model, but the barrier for TS27 is slightly increased to 27.2 kJ mol^{-1}. A conformer, P10, of P7 is able to be produced here from IM34 that will spontaneously dissociate and recombine a H_2O molecule *via* P9 to produce IM35, and then to isomerize into IM36, a species of hydrated P10, *via* TS22 with a barrier of 64.0 kJ mol^{-1}. The barrier of the conformers linked directly (*i.e.*, without H_2O) by 'TS22' in ref. [1] was also reported by 33.7 kJ mol^{-1}, implying that a water molecule does not catalyze the conformational transition.

The additional reactions of P7+H_2O are shown in panel (b) of Fig. 12 where complexes IM45 and IM30 are first formed. For the channels to produce the final product N(9)H+H_2O, the highest barrier, 76.0 kJ mol^{-1}, is found in the transition of IM65 to IM66 *via* TS41. The next highest, 72.2 kJ mol^{-1}, is in IM57 to IM60 *via* TS37, which is already lower than the lowest barrier, 74.8 kJ mol^{-1}, in the transitions of N(7)H+H_2O to P7+H_2O or to P10+H_2O discussed previously. This implies that even lower barriers can be found. Actually among all the paths in Fig. 12(b), there exist two comparable favored channels that have the highest barriers of only 58.6 kJ mol^{-1} for IM52 to IM53 and 59.4 kJ mol^{-1} for IM58 to IM59. Therefore, the rate determining step should be the transition of IM1 to IM26 in Fig. 12(a) that has the barrier of 74.8 kJ mol^{-1}. Considering the next lowest

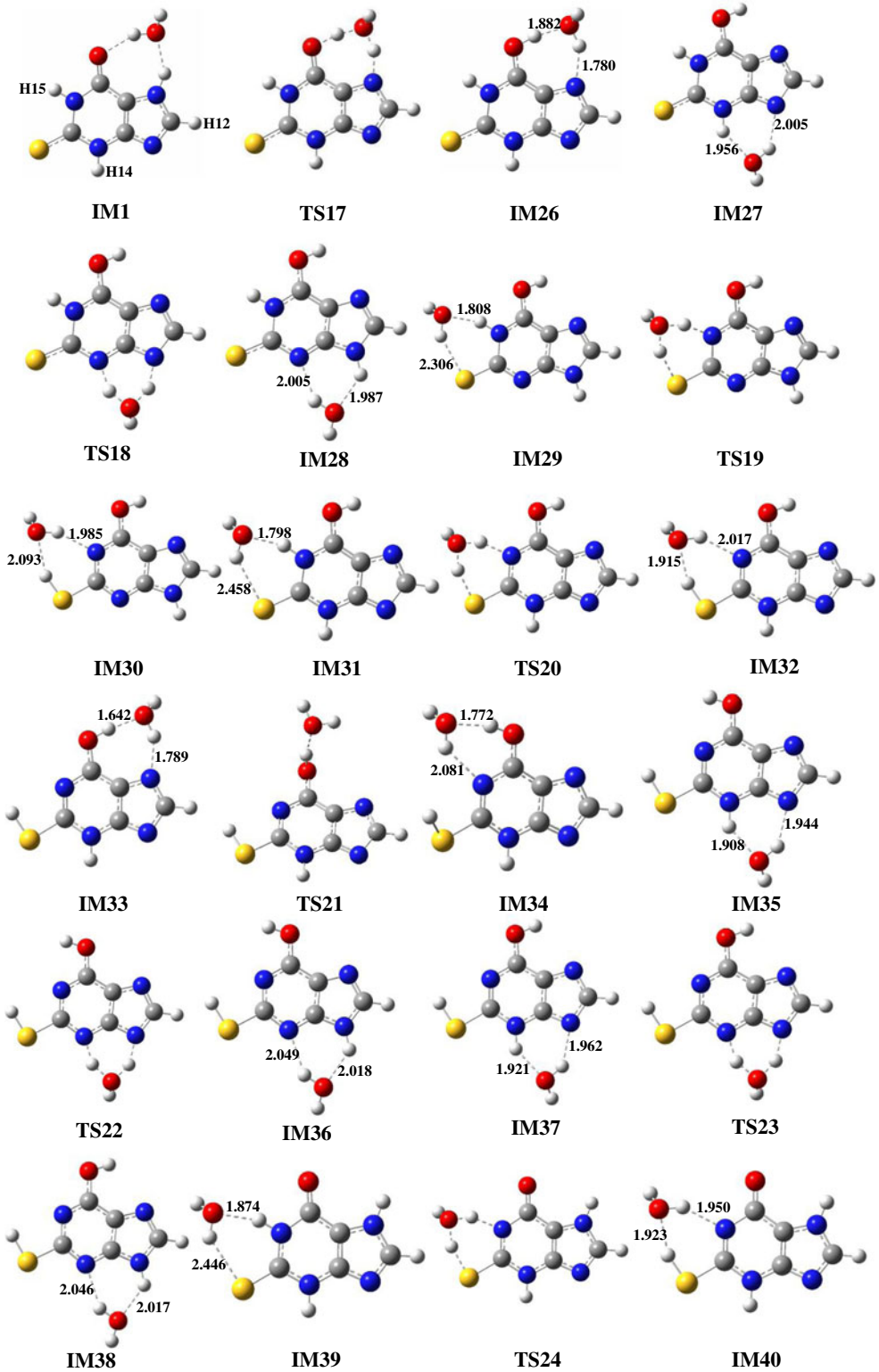

Fig. 10 Optimized geometries of the complexes and transition states associated with the proton transfers *via* the O, S and N atoms of pyrimidine ring for the one water-assisted process of 2-thioxanthine tautormerizations. Bond distances are in Å

necessary barrier, 96.8 kJ mol^{-1} for IM39 to IM40, being 22.0 kJ mol^{-1} higher (or the rate branching ratio being about 1.4×10^{-4} estimated with the Boltzmann factor at 298.15 K), the most feasible path in the one water catalysis microsolvent environment is thus N(7)H+H_2O→IM1→IM26→P5+H_2O→IM31→IM32→P8+H_2O→IM33→IM34→P9+H_2O→

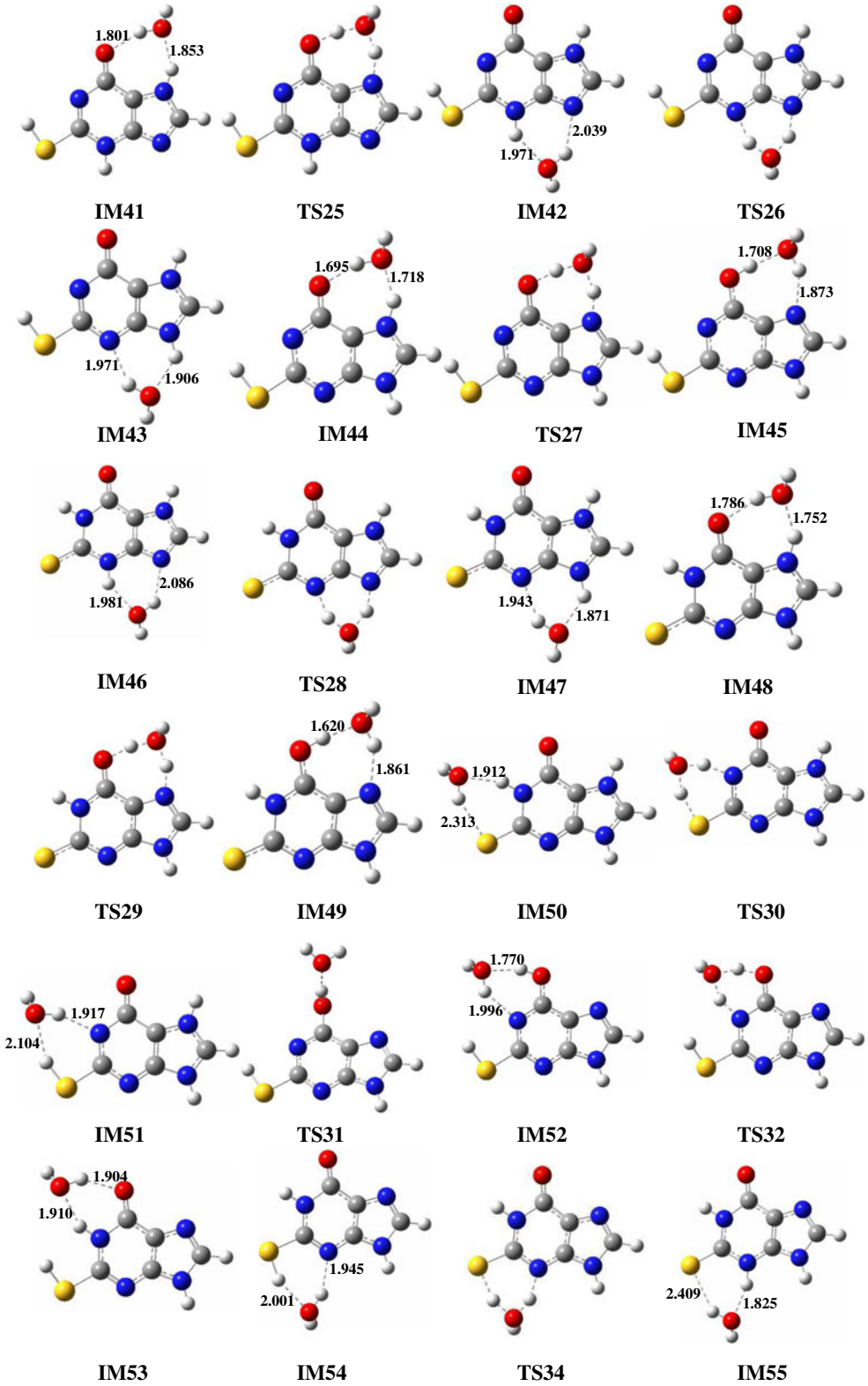

Fig. 10 (continued)

IM35→IM36→P10+H_2O→IM56→IM57→P16+H_2O→IM58→IM59→P15+H_2O→IM54→IM55→N(9)H+H_2O, where the path may also branch from the seventh step P8+H_2O into P8+H_2O→IM37→IM38→P7+H_2O→IM45→IM52→IM53→P14+H_2O→P14→P15→P15+H_2O as the competitive reactions. These

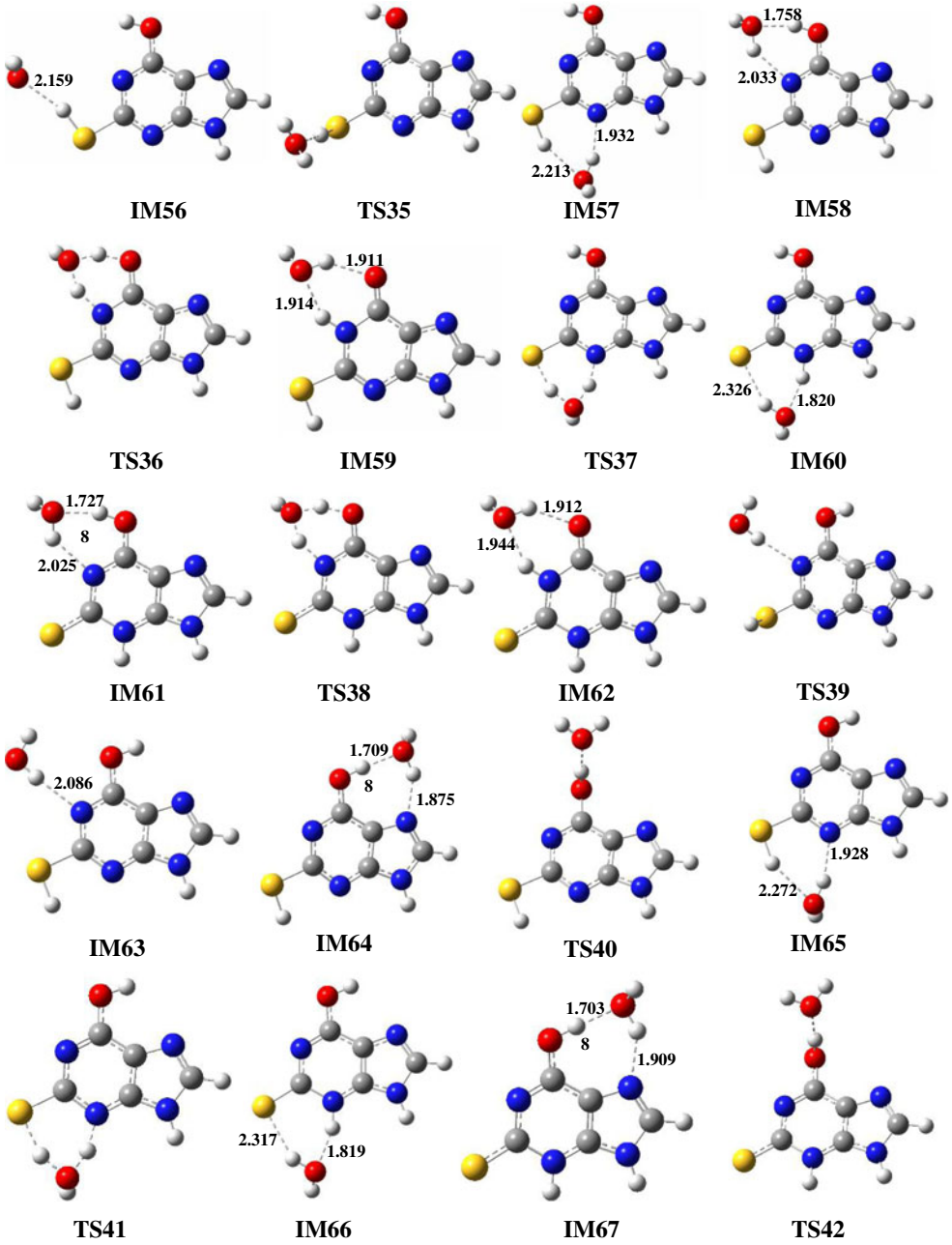

Fig. 10 (continued)

latter reactions are also in the most favorable channel found with the PCM solvent model. Therefore, the rate determining step is for the transition of IM1 to IM26 *via* TS17 with the barrier of 58.0 kJ mol^{-1} which is obviously lower by 16.8 kJ mol^{-1} than that, 74.8 kJ mol^{-1}, in the microsolvent phase. Although either 74.8 or 58.0 kJ mol^{-1} is a moderate barrier for a chemical reaction to be proceeded at room temperature, the tautomerization is easier in the water solvent in the presence of a water molecule.

In this pathway, the concentrations for all the intermediates are increased in the aqueous phase (Supplement 5) but only IM39 and IM46 are expected observable due to a relative concentration larger than 1 ppm by 8.3×10^{-6} and 9.0×10^{-6} with respect to the most stable IM21.

Proton transferring reactions via the O, S and N atoms in the pyrimidine ring facilitated by two water molecules

Very similar to the one water catalysis reactions, the proton transfers *via* the O, S and N atoms of pyrimidine ring with the existence of two water molecules were examined. The optimized structures for all 47 stable complexes and 25 transition states involved in these pathways are summarized in Fig. 13. The energy profiles

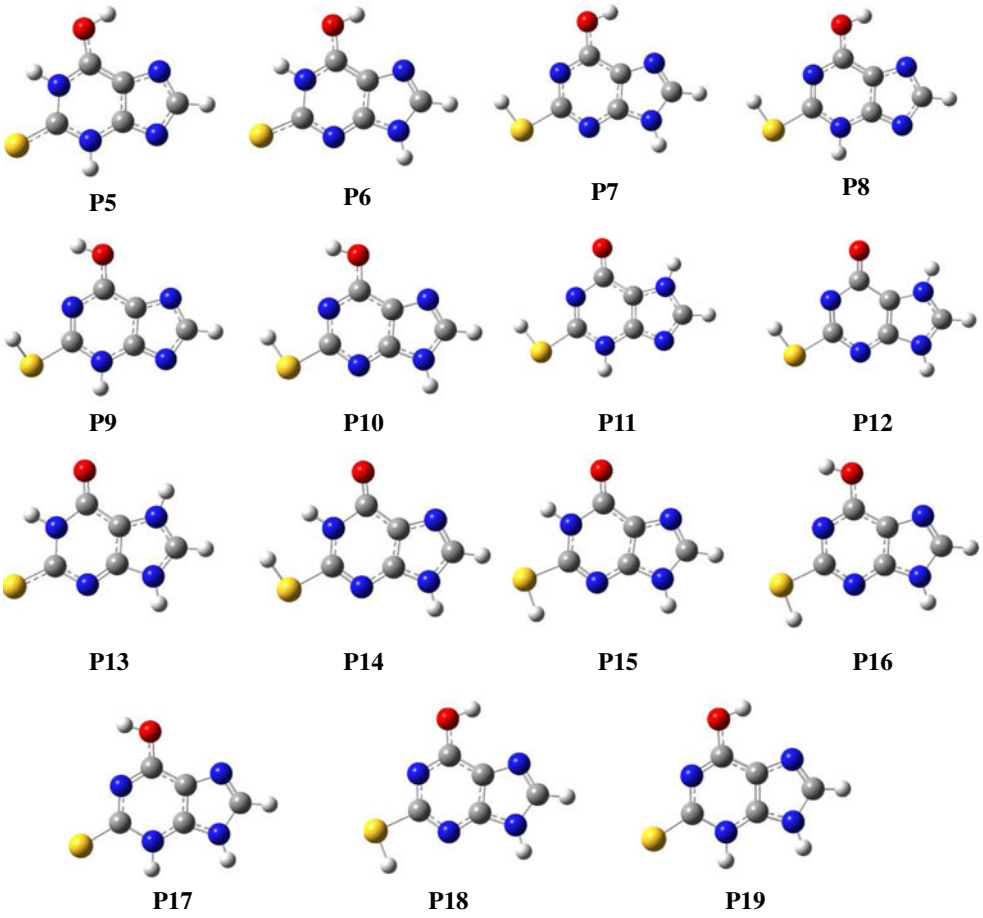

Fig. 11 Optimized structure of the isolated intermediates associated with the proton transfers *via* the O, S and N atoms of pyrimidine ring in the process of 2-thioxanthine tautomerizations

of the two water assistant reaction pathways are illustrated in Fig. 14.

Figure 14 is also separated into two panels: (a) is for di-hydrated N(7)H to di-hydrated P7 or P10 and (b) is continued for di-hydrated P7 to the product N(9)H. Figure 14(a) shows that the first group of the higher barriers is in the first transition of the hydrated reactant *via* TS43, TS50 and TS54, and all the transitions are intermolecular concerted triple proton transfers between thione-keto tautomers and two water molecules. The second group of the higher barriers appears in the middle of the panel that corresponds to the transitions between thione-thiol tautomers and two water molecules *via* TS44 and TS46, between thiol-keto tautomers and two water molecules *via* TS51 and TS52, and between thione-keto tautomers and two water molecules *via* TS55 and TS56. The last group is at the rear end of the panel that corresponds to the transitions of the thione-thiol tautomers *via* TS45, thiol-enol tautomers *via* TS47 and TS49, and thiol-keto tautomers *via* TS53.

It is shown in panel (a) that the higher barriers in the first group are in the necessary reaction pathways, where the highest barrier is 94.7 kJ mol^{-1} for IM81 to IM82 and the lowest is 82.1 kJ mol^{-1} for IM21 to IM68 *via* TS43. This barrier, 82.1 kJ mol^{-1}, is also the highest one among the favorable reaction steps followed. Compared with that in the previous mono-hydration process (*via* TS17), the present value is 7.3 kJ mol^{-1} higher, implying that an additional water molecule does not significantly enhance the catalytic property of the proton transfer. The feasible pathway is thus $N(7)H+2H_2O \rightarrow IM21 \rightarrow IM68 \rightarrow P5+2H_2O \rightarrow IM69 \rightarrow IM70 \rightarrow P6+2H_2O \rightarrow IM71 \rightarrow IM72 \rightarrow P7+2H_2O$ and the higher barriers are within the transitions of IM21 to IM68 *via* TS43 by 82.1, IM69 to IM70 *via* TS44 by 64.4 and IM71 to IM72 *via* TS45 by 70.3 kJ mol^{-1}. The next possible pathway may also be drawn by $N(7)H+2H_2O \rightarrow IM21 \rightarrow IM68 \rightarrow P5+2H_2O \rightarrow IM73 \rightarrow IM74 \rightarrow P8+2H_2O \rightarrow IM79 \rightarrow IM80 \rightarrow P7+2H_2O$, which branches at the third step of the previous channel. The highest barrier is also in the transition of IM21 to IM68 but the followed highest barrier, 74.7 kJ mol^{-1} for IM73 to IM74, is only 4.4 kJ mol^{-1} higher than that in the previous channel. Within this pathway at P8+$2H_2O$, the reaction may branch into $IM75 \rightarrow IM76 \rightarrow P9+2H_2O \rightarrow IM77 \rightarrow IM78 \rightarrow P10+2H_2O$ to produce the conformer, P10, of P7 with the highest barrier of 68.9 kJ mol^{-1} for IM75 to IM76 *via* TS47 which is the only possible channel since another path to produce P10 has a barrier of 94.7 kJ mol^{-1} (or a Boltzmann factor of 3.0×10^{-5}) for IM81 to IM82 *via* TS50.

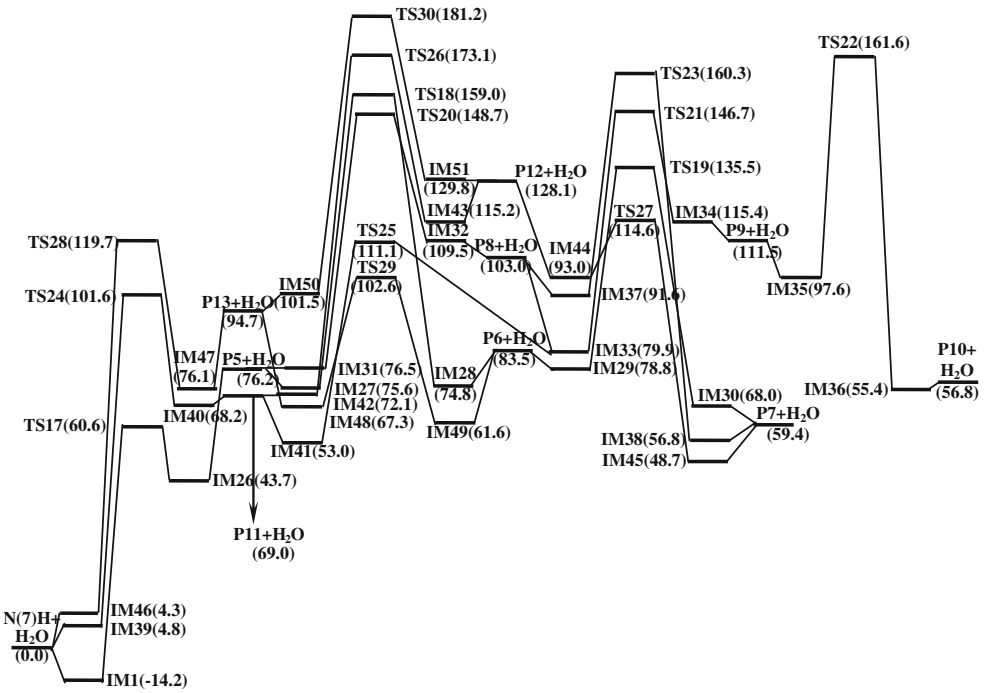

(a) from N(7)H+H_2O to P7 or P10+H_2O

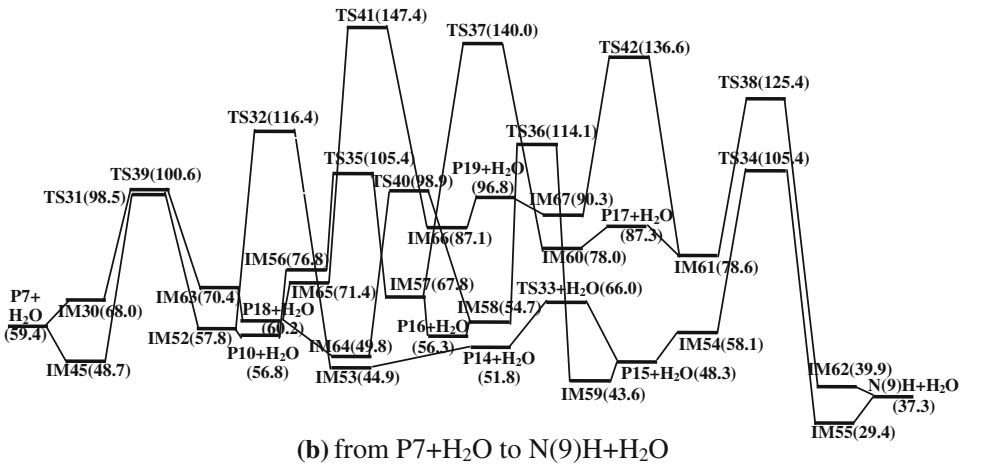

(b) from P7+H_2O to N(9)H+H_2O

Fig. 12 Reaction pathways for one water molecule assisted proton transfer tautomerization processes of 2-thioxanthine *via* the O, S and N atoms of pyrimidine ring. Energy or energy barrier is in kJ mol^{-1} and is the Gibbs free energy at 298.15 K obtained with B3LYP/aug-cc-pVTZ//B3LYP/6-311+G**. **a** is the profile from N(7)H+H_2O to P7+H_2O or to P10+H_2O and **b** continues from P7+H_2O to N(9)H+H_2O

By involving the PCM solvent model, however, the highest barrier, 82.1 kJ mol^{-1}, is decreased to 47.4 kJ mol^{-1}, implying the importance of the solvent effect. In considering the long-range solvent, an even lower barrier, 44.0 kJ mol^{-1}, is found in the transition of IM89 to IM90 *via* TS54 instead of that found previously at the very beginning of the reaction. Therefore, the most feasible reaction pathway is N(7)H+$2H_2O$→IM89→IM90→P13+$2H_2O$→IM91→IM92→P6+$2H_2O$→IM71→IM72→P7+$2H_2O$, and the highest barrier 44.0 kJ mol^{-1} in this channel is also 14.0 kJ mol^{-1} lower than that in the one water catalysis process.

Figure 14(b) continues the reactions of P7+$2H_2O$ and the most feasible pathway is P7+$2H_2O$→IM88→IM95→P10+$2H_2O$→IM96→IM97→P14+$2H_2O$→P14→P15→P15+$2H_2O$→IM98→IM8→N(9)H+$2H_2O$, in which, the highest barrier, 57.3 kJ mol^{-1}, is in the transition of IM96 to IM97 *via* TS58 and the next highest, 52.5 kJ mol^{-1}, is in IM98 to IM8 *via* TS59. Another competitive pathway branches from P10+$2H_2O$ into (P10+$2H_2O$)→IM99→IM100→P16+$2H_2O$→IM101→IM102→P15+$2H_2O$, and P15 follows the same steps as shown above. The highest barrier, 58.6 kJ mol^{-1} for IM101 to IM102 *via* TS61, is found. Obviously, all the highest barriers are at least 23.4 kJ

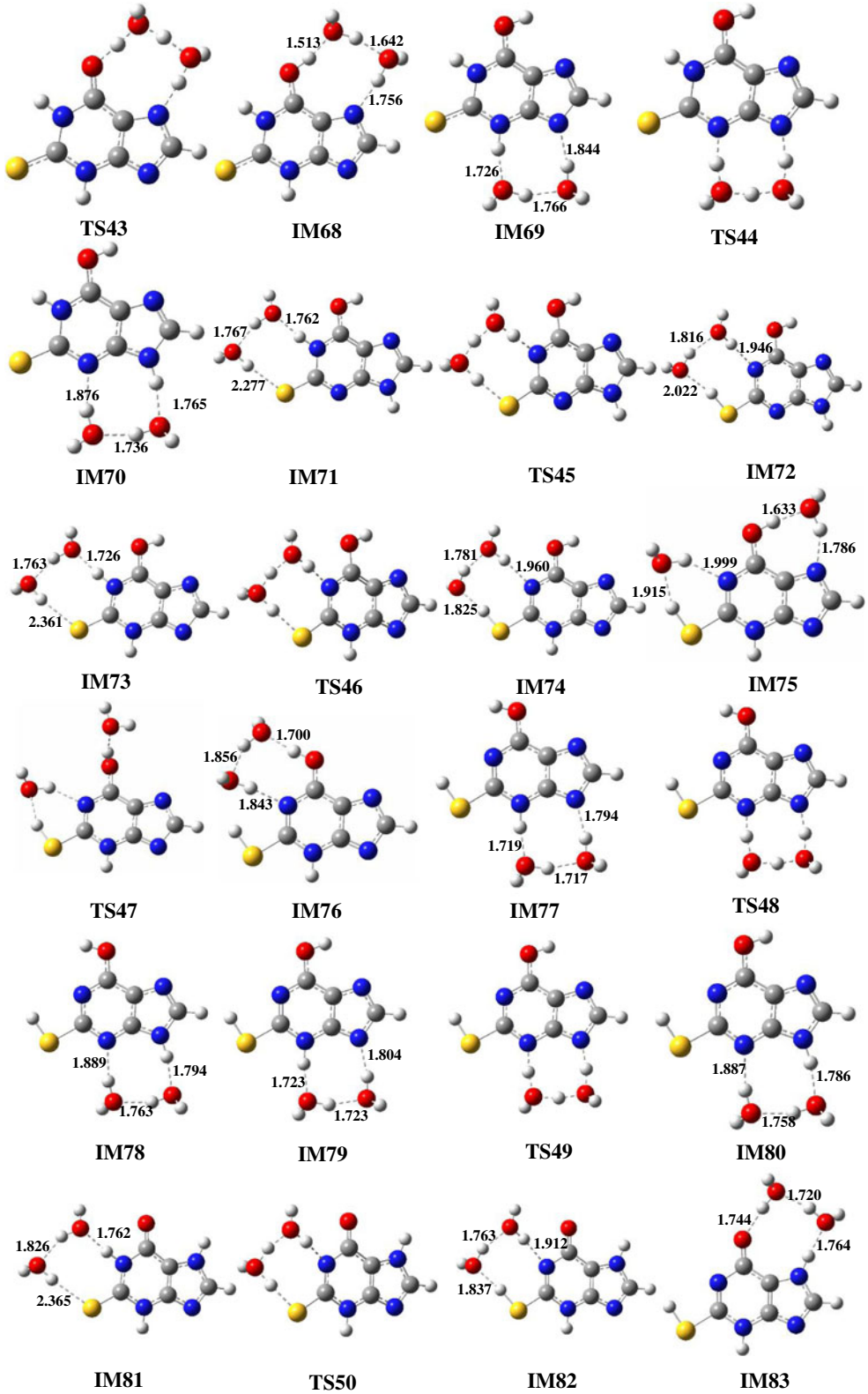

Fig. 13 Optimized geometries of the complexes and transition states associated with the proton transfers *via* the O, S and N atoms of pyrimidine ring for the two water-assisted process of 2-thioxanthine tautormerizations. Bond distances are in Å

mol^{-1} lower than that, 82.1 kJ mol^{-1}, in the necessary reaction step shown in panel (a).

By involving the PCM solvent model, the highest barrier, 57.3 kJ mol^{-1}, is decreased to 32.2 kJ mol^{-1}

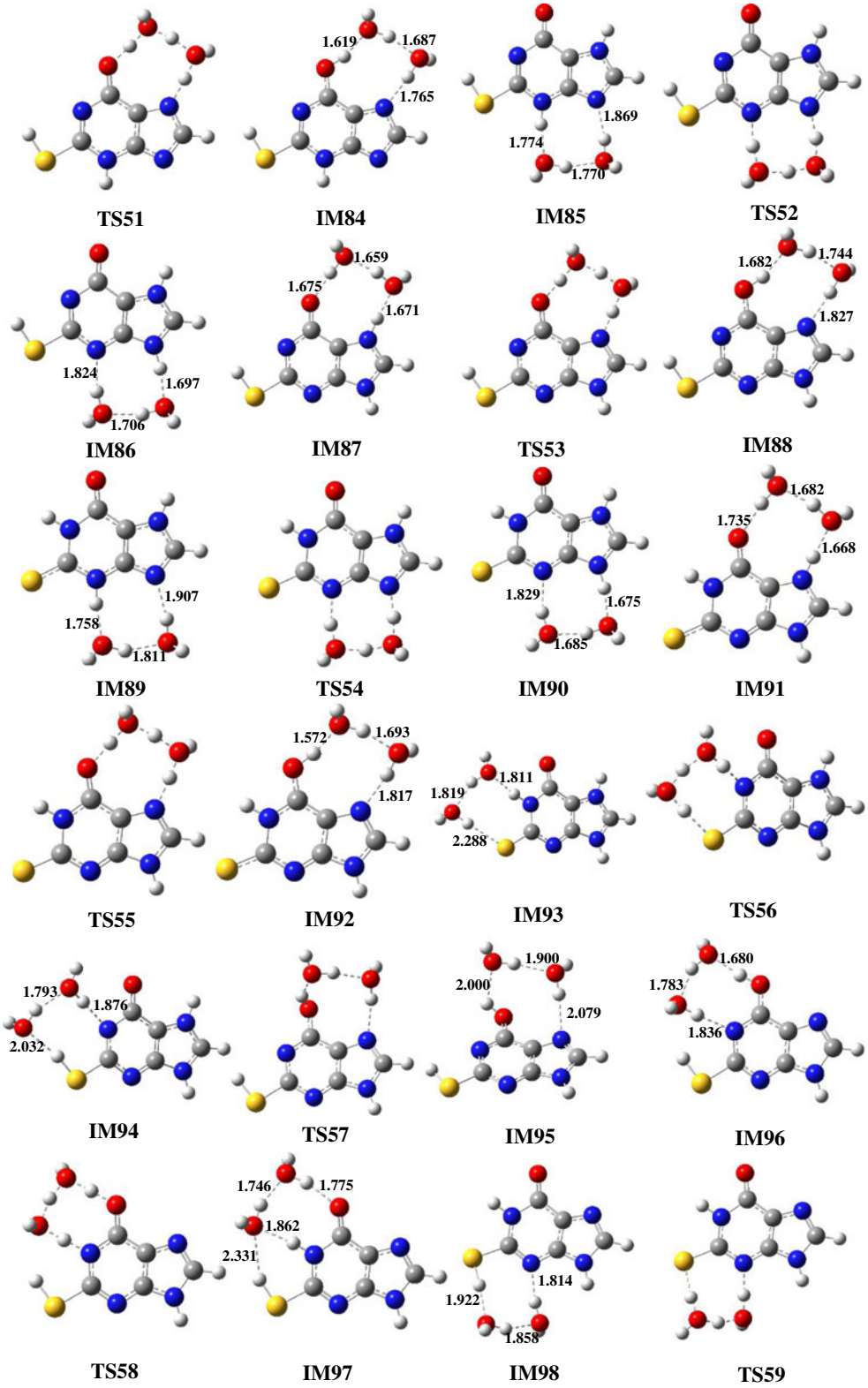

Fig. 13 (continued)

and the barrier for IM88 to IM95 *via* TS57 is slightly increased from 31.8 into 34.9 kJ mol^{-1}. Hence the most feasible path is $P7+2H_2O \rightarrow IM107 \rightarrow IM108 \rightarrow P18+2H_2O \rightarrow IM111 \rightarrow IM112 \rightarrow P19+2H_2O \rightarrow IM113 \rightarrow IM114 \rightarrow P17+2H_2O \rightarrow IM105 \rightarrow IM106 \rightarrow N(9)H+2H_2O$. Other pathways are also possible *via* TS65, TS66, TS61,

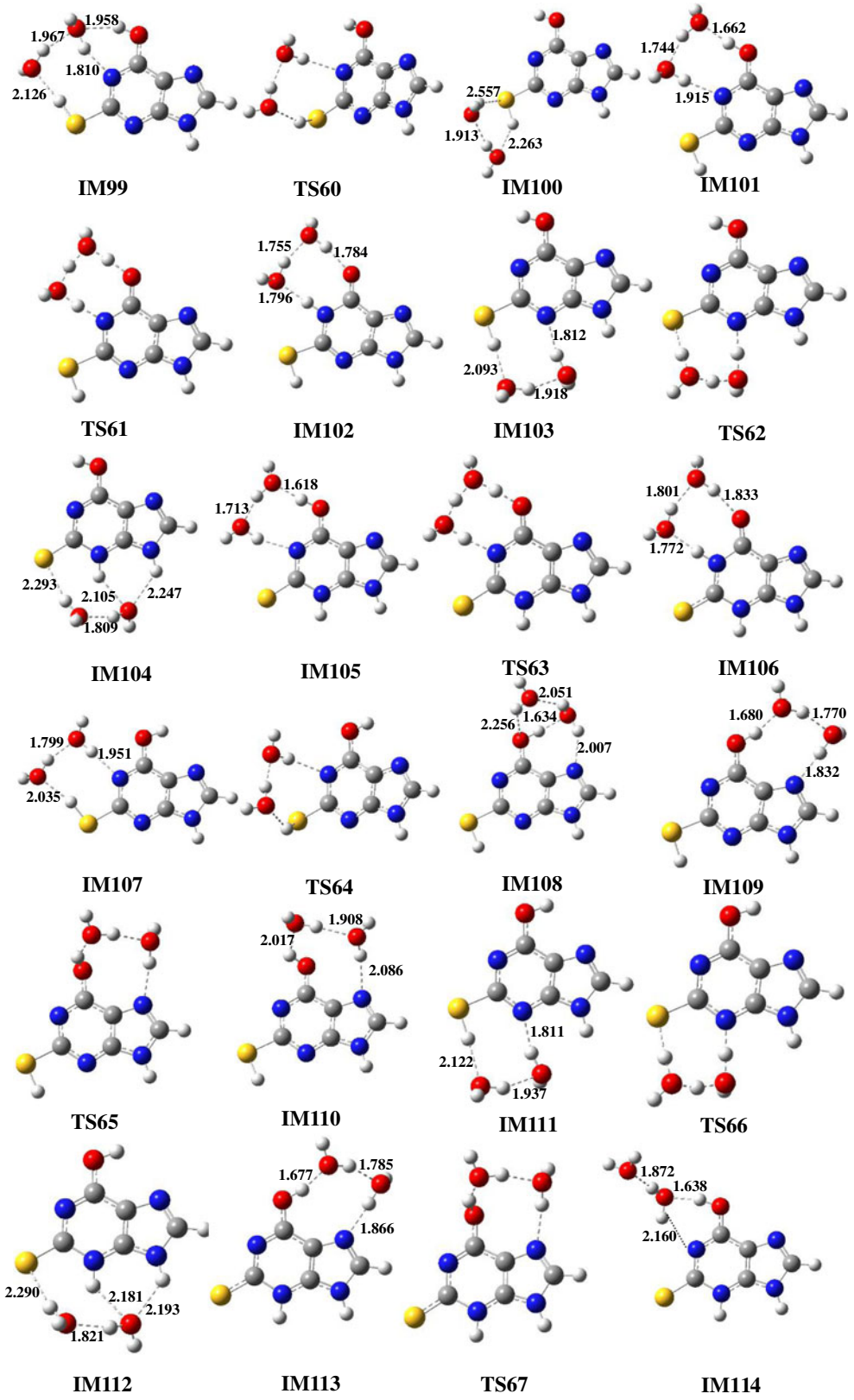

Fig. 13 (continued)

TS62, TS67, TS59 and TS63 with the highest barrier of only 33.6 kJ mol^{-1}.

Combining the discussions for panel (a) and (b), the most feasible reaction pathway in the di-hydrated microsolvent is

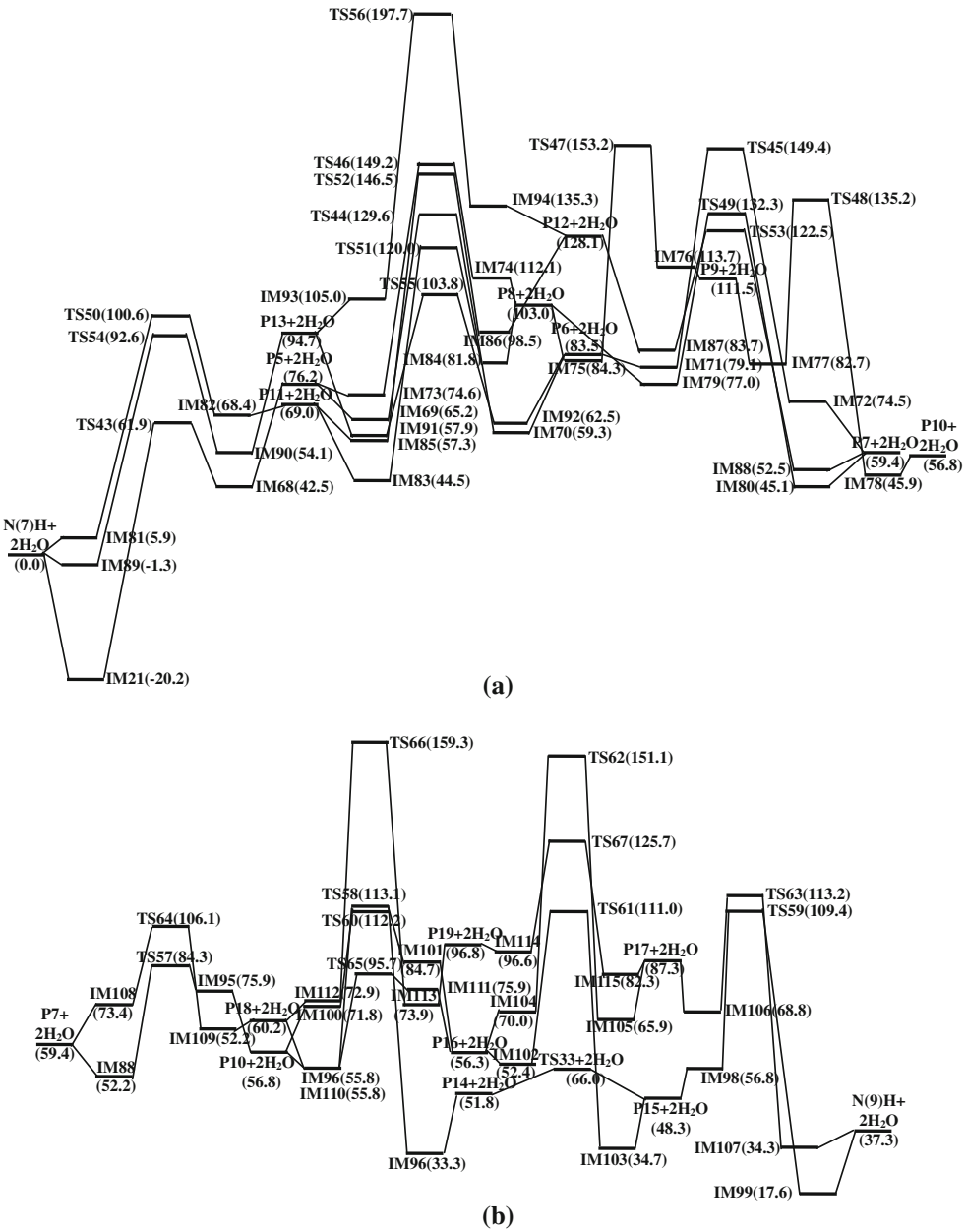

Fig. 14 **a** and **b** are reaction pathways for two water molecule assisted proton transfer tautomerization processes of 2-thioxanthine *via* the O, S and N atoms of pyrimidine ring. Energy or energy barrier is in kJ mol^{-1} and is the Gibbs free energy at 298.15 K obtained with B3LYP/aug-cc-pVTZ//B3LYP/6-311+G**. **a** is the profile from N(7)H+2H_2O to P7+2H_2O or to P10+2H_2O and **b** continues from P7+2H_2O to N(9)H+2H_2O

N(7)H+2H_2O→IM21→IM68→P5+2H_2O→IM69→IM70→P6+ 2H_2O→IM71→IM72→P7+2H_2O→IM88→IM95→P10+2H_2O→IM96→IM97→P14+2H_2O→P14→P15→P15+2H_2O→IM98→IM8→N(9)H+2H_2O, in which, the highest barrier, 82.1 kJ mol^{-1}, is in the transition of IM21 to IM68 *via* TS43. However, in the PCM solvent model, the most feasible reaction pathway is changed into N(7)H+2H_2O→IM89→IM90→P13+2H_2O→IM91→IM92→P6+2H_2O→IM71→IM72→P7+2H_2O→IM107→IM108→P18+2H_2O→IM111→IM112→P19+2H_2O→IM113→IM114→P17+2H_2O→IM105→IM106→N(9)H+2H_2O with the highest barrier of 44.0 kJ mol^{-1}. Therefore, the tautomerization of the 2-thioxanthine in water solution should follow the mechanism with the presence of two water molecules as the microsolvent catalysis within the environment of long range solvent that has a highest energy barrier of only 44.0 kJ mol^{-1}.

In this pathway, all the intermediates IM81, IM89, IM90, IM91 and IM106 are possible to co-existed with IM21 in the aqueous phase due to larger relative concentrations of 2.1×10^{-3}, 0.2, 2.1×10^{-5}, 4.5×10^{-5} and 2.6×10^{-4}. Especially, IM89, a structure having two water molecules located on the other edge side of **N(7)H**, has a high concentration of 20 % with respect to IM21. This might predict that even some stable complexes could be found within the 3H_2O and 4H_2O models. This must an interesting subject that needs to be studied in our further work.

Conclusions

The reaction pathways of the 2-thioxanthine proton transfer tautomerization were investigated theoretically with density functional theory both in the microsolvent (mono-hydration and di-hydration) and the long-range solvent PCM models. This involves 115 reaction complexes and 67 transition states. Molecular geometries were determined with B3LYP/6-311+G** calculations and the energies were refined with a larger base set at B3LYP/aug-cc-pVTZ level. Gibbs free energy corrections at 298.15 K were obtained with the standard statistical thermodynamics by using the optimized geometries and the scaled theoretical frequencies. The energy barriers and the reaction energies were examined by using the Gibbs free energies at 298.15 K. The results show that proton transfer *via* the C8 atom on the imidazole ring has the lowest barrier of 220.1 kJ mol^{-1} with mono-hydration and 159.7 kJ mol^{-1} with di-hydration catalysis without the PCM long-range solvent, while the respective data are 208.5 and 120.6 kJ mol^{-1} with PCM. The transfer *via* the bridged C4 and C5 atoms between pyrimidine and imidazole rings has the lowest barrier of 251.7 kJ mol^{-1} with mono-hydration and 204.0 kJ mol^{-1} with di-hydration microsolvent without the PCM model, while they are 212.4 and 163.4 kJ mol^{-1} with PCM. The direct proton transfer with one or two water molecules catalysis has a sole barrier of 265.2 or 184.0 kJ mol^{-1}, respectively, while the barrier is reduced to 181.1 or 83.9 kJ mol^{-1} with PCM. The transfer *via* the N, O and S atoms on the pyrimidine ring has the lowest barrier of 74.8 kJ mol^{-1} for mono-hydration and 82.0 kJ mol^{-1} for di-hydration without the PCM model. Each of these barriers is much lower in the long-range solvent and the lowest barrier is 58.0 kJ mol^{-1} for mono-hydration and is 44.0 kJ mol^{-1} for di-hydration. Therefore, the most feasible pathway is identified as di-hydrated process combined with the long-range solvent model by $N(7)H+2H_2O \rightarrow IM89 \rightarrow IM90 \rightarrow P13+2H_2O \rightarrow IM91 \rightarrow IM92 \rightarrow P6+2H_2O \rightarrow IM71 \rightarrow IM72 \rightarrow P7+2H_2O \rightarrow IM107 \rightarrow IM108 \rightarrow P18+2H_2O \rightarrow IM111 \rightarrow IM112 \rightarrow P19+2H_2O \rightarrow IM113 \rightarrow IM114 \rightarrow P17+2H_2O \rightarrow IM105 \rightarrow IM106 \rightarrow N(9)H+2H_2O$. The highest barrier, 44.0 kJ mol^{-1}, is in the transition of IM89 to IM90 *via* TS54. This barrier is also much lower than that, 295.0 kJ mol^{-1}, in the intramolecular proton transfer without water catalysis examined previously in ref. [1]. The present result predicts that the tautomerization reactions are very feasible at room temperature in the aqueous phase and is consistent with the experiments, although the experimental activation energy has not been reported. This work also found that the energies of all the similar intermediates with two water microsolvent are lower than those with one water molecule. IM21 [**N(7)H-**$2H_2O$] is the most stable complex either with or without the long-range solvent. In the aqueous solution, the possible co-existing species are the monohydrated IM1, IM9, IM39 and IM46, and the di-hydrated IM5, IM8, IM13, IM16, IM81, IM89, IM90, IM91 and IM106 complexes that have a relative concentration larger than 10^{-6} (1 ppm) with respect to IM21.

Acknowledgments Part of the calculations were performed in the High Performance Computation Center of the Northwestern Polytechnical University. Support by the Basic Research Foundation of Northwestern Polytechnical University (Grant No. JC201269) and Wenli Special Foundation of Xi'an Science Technology Bureau (CXY1134WL13) is greatly acknowledged.

References

1. Ren HJ, Su KH, Liu Y, Wang X, Wang YL, Xiao J (2012) Proton transfer tautomerization mechanisms of 2-thioxanthine. Comput Theor Chem 982:40–46
2. Speina E, Ciela JM, Grziewicz MA, Laval J, Kazimierczuk Z, Tudek B (2005) Inhibition of DNA repair glycosylases by base analogs and tryptophan pyrolysate, Trp-P-1. Acta Biochim Pol 52:167–178
3. Elgemeie GH (2003) Thioguanine, mercaptopurine: their analogues and nucleosides as antimetabolites. Curr Pharm Des 9:2627–2642
4. Kouni MH (2003) Potential chemotherapeutic targets in the purine metabolism of parasites. Pharmacol Ther 99:283–309
5. Papakostas K, Georgopoulou E, Frillingos S (2008) Cysteine-scanning analysis of putative Helix XII in the YgfO xanthine permease. J Biol Chem 283:13666–13678
6. Mautner HG, Bergson G (1963) Some remarks on position-conditioned differences of the ultraviolet spectra and chemical reactivities of disubstituted pyrimidines and purines. Acta Chem Scand 17:1694–1704
7. Twanmoh LM, Wood HB, Driscoll JS (1973) NMR spectral characteristics of N-H protons in purine derivatives. J Heterocycl Chem 10:187–190
8. Civcir PU (2001) Tautomerism of 2-thioxanthine in the gas and aqueous phases using AM1 and PM3 methods. J Mol Struct (THEOCHEM) 546:163–173
9. Li BZ (2004) Density functional theory calculations on 2-thioxanthine. Acta Phys Chim Sin 20:1455–1458
10. Ahn DS, Lee S, Bongsoo K (2004) Solvent-mediated tautomerization of purine: single to quadruple proton transfer. Chem Phys Lett 390:384–388
11. Jeon IS, Ahn DS, Park SW, Lee S, Kim SK (2005) Structures and isomerization of serine in aqueous solution: computational study. Chem Phys Lett 403:72–76
12. Lee KM, Park SW, Jeon IS, Lee BR, Ahn DS, Lee SB (2005) Density functional theory study of acetonitrile-water clusters: structures and Infrared frequency shifts. Bull Korean Chem Soc 26:909–915
13. Park SW, Im S, Lee S, Desfrancois C (2007) Structure and stability of glycine-$(H_2O)_3$ cluster and anion: zwitterion vs. canonical glycine. Int J Quantum Chem 107:1316–1327
14. Yoon I, Seo K, Lee S, Lee Y, Kim B (2007) Conformational study of tyramine and its water clusters by laser spectroscopy. J Phys Chem A 111:1800–1807
15. Baymak MS, Vercoe KL, Zuman P (2005) Strong covalent hydration of terephthalaldehyde. J Phys Chem B 109:21928–21929
16. Ahn DS, Kang AR, Lee S, Kim B, Kim SK, Neuhauser D (2005) On the stability of glycine-water clusters with excess electron: implications for photoelectron. J Chem Phys 122:084310–084319

17. Gorb L, Leszczynski J (1998) Intramolecular proton transfer in mono- and dihydrated tautomers of guanine: an ab initio Post Hartree-Fock study. J Am Chem Soc 120:5024–5032
18. Kastas G (2012) Investigating the prototropic tautomerism in (E)-2-[(4-fluorophenyl)iminomethyl]- 5-methoxyphenol compound for solid state and solvent media by experimental and quantum computational tools. J Mol Struct 1017:38–44
19. Iglesias E (2003) Tautomerization of 2-acetylcyclohexanone.1.characterization of keto-enol/enolate equilibria and reaction rates in water. J Org Chem 68:2680–2688
20. Shen Z, Zhang YL, Jin FM, Zhou XF, Kishita A, Tohji K (2010) Hydrogen-transfer reduction of ketones into corresponding alcohols using formic acid as a hydrogen donor without a metal catalyst in high-temperature water. Ind Eng Chem Res 49:6255–6259
21. Riley BT, Long FA (1962) Long, deuterium isotope and solvent effects on the kinetics of the keto-enol interconversion of 2-acetylcyclohexanone. J Am Chem Soc 84:522–526
22. Ahn DS, Lee S, Kim B (2004) Solvent-mediated tautomerization of purine: single to quadruple proton transfer. Chem Phys Lett 390:384–388
23. Kim HS, Ahn DS, Chung SY, Kim SK, Lee S (2007) Tautomerization of adenine facilitated by water: computational study of microsolvation. J Phys Chem A 111:8007–8012
24. Okovytyy SI, Sviatenko LK, Gaponov AA, Kasyan LI, Tarabara IN, Leszczynski J (2010) DFT study on tautomerism of dihydro-2*H*-1,5-benzodiazepin-2-ones and dihydro-2*H*-1,5-benzodiazepine-2-thiones. Eur J Org Chem 2:280–291
25. Yuan XX, Wang YF, Wang X, Chen WB, Fossey JS, Wong NB (2010) An ab initio and AIM investigation into the hydration of 2-thioxanthine. Chem Cent J 4:1–19
26. Balta B, Aviyente V (2003) Solvent effects on Glycine. I. A supermolecule modeling of tautomerization via intramolecular proton transfer. J Comput Chem 24:1789–1802
27. Balta B, Aviyente V (2004) Solvent effects on Glycine II. Water-assisted tautomerization. J Comput Chem 25:690–703
28. Frisch MJ, Trucks GW, Schlegel HB, Scuseria G.E, Robb MA, Cheeseman JR, Scalmani G., Barone, V, Mennucci B, Petersson GA, Nakatsuji H, Caricato M, Li X, Hratchian HP, Izmaylov AF, Bloino J, Zheng G, Sonnenberg JL, Hada M, Ehara M, Toyota K, Fukuda R, Hasegawa J, Ishida M, Nakajima T, Honda Y, Kitao O, Nakai H, Vreven T, Montgomery JA Jr, Peralta JE, Ogliaro F, Bearpark M, Heyd, JJ, Brothers E, Kudin KN, Staroverov VN, Kobayashi R, Normand J, Raghavachari K, Rendell A, Burant JC, Iyengar SS, Tomasi J, Cossi M, Rega N, Millam JM, Klene M, Knox JE, Cross JB, Bakken V, Adamo C, Jaramillo J, Gomperts R, Stratmann RE, Yazyev O, Austin AJ, Cammi R, Pomelli C, Ochterski JW, Martin RL, Morokuma K, Zakrzewski VG., Voth GA, Salvador P, Dannenberg JJ, Dapprich S, Daniels AD, Farkas O, Foresman JB, Ortiz JV, Cioslowsk J, Fox DJ (2009) Gaussian 09, Revision A.02, Gaussian Inc., Wallingford, CT
29. Becke AD (1993) Density-functional thermochemistry. III. The role of exact exchange. J Chem Phys 98:5648–5652
30. Chuang CH, Lien MH (2004) Ab initio study on the effects of the substituent and the functional group on the isomerization of H3CC(X)Y and H2C(X)CHY(Y=SiH2, PH, S; X=H, CH3, NH2, OH, F). J Phys Chem A 108:1790–1798
31. Li P, Bu Y (2004) Investigation of double proton transfer behavior between glycinamide and formamide using density functional theory. J Phys Chem A 108:10288–10295
32. Nagy PI, Tejada FR, Messer WS (2005) Theoretical studies of the tautomeric equilibria for five-member n-heterocyles in the gas phase and in solution. J Phys Chem B 109:22588–22602
33. Lamsabhi AM (2008) Specific hydration effects on oxo−thio triazepine derivatives. J Phys Chem A 112:1791–1797
34. Miertuš S, Scrocco E, Tomasi J (1981) Electrostatic interaction of a solute with a continuum. A direct utilization of ab initio molecular potentials for the prevision of solvent effects. Chem Phys 55:117–129
35. Miertuš S, Tomasi J (1982) Approximate evaluations of the electrostatic free energy and internal energy changes in solution processes. Chem Phys 65:239–245
36. Pascual-Ahuir JL, Silla E, Tuñón I (1994) GEPOL: an improved description of molecular-surfaces. 3. A new algorithm for the computation of a solvent-excluding surface. J Comput Chem 15:1127–1138
37. Cossi M, Barone V (2000) Solvent effect on vertical electronic transitions by the polarizable continuum model. J Chem Phys 112:2427–2435
38. Tomasi J, Mennucci B, Cammi R (2005) Quantum mechanical continuum solvation models. Chem Rev 105:2999–3093
39. Jeffrey P, Merrick DM, Leo R (2007) An evaluation of harmonic vibrational frequency scale factors. J Phys Chem A 111:11683–11700
40. Barone V, Cossi M (1998) Quantum calculation of molecular energies and energy gradients in solution by a conductor solvent model. J Phys Chem A 102:1995–2001
41. Cossi M, Rega N, Scalmani G, Barone V (2003) Energies, structures, and electronic properties of molecules in solution with the C-PCM solvation model. J Comput Chem 24:669–681
42. Marenich AV, Cramer CJ, Truhlar DG (2009) Universal solvation model based on solute electron density and on a continuum model of the solvent defined by the bulk dielectric constant and atomic surface tensions. J Phys Chem B 113:6378–6396